Environmental Science: Atmospheres

ROYAL SOCIETY OF CHEMISTRY

PAPER

View Article Online
View Journal | View Issue

Cite this: *Environ. Sci.: Atmos.*, 2025, **5**, 25

Exploring the influence of physical and chemical factors on new particle formation in a polluted megacity†

Umer Ali,[a] Vikram Singh,*[a] Mohd Faisal,[a] Mayank Kumar[b] and Shahzad Gani *[cd]

Delhi is one of the most polluted regions in the world, yet studies focusing simultaneously on atmospheric aerosol particle size distribution (PSD) and chemical composition, as well as their inter-relationship, are still lacking. Additionally, the high condensation sink (CS) in Delhi has drawn less attention to new particle formation (NPF) and the role of chemical composition. This study explored the intricate interplay among particle size distribution, meteorology, and chemical composition within the atmospheric environment of Delhi. Our findings reveal pronounced seasonal variations in the particle number and mass concentration levels following variations in atmospheric conditions and emission sources across different seasons. Furthermore, we identified condensation sink as a primary factor governing the NPF, with no NPF event observed when daytime CS was above 0.06 s^{-1}. While precursors such as H_2SO_4 and NH_3 were abundant, they did not appear to be limiting factors for NPF. However, due to the lack of direct measurements of sub-10 nm particles and precursor gases such as H_2SO_4, amines, and organic vapours, the conclusions regarding the role of chemical precursors remain speculative. Furthermore, on days with comparable condensation sinks, the chemical composition exhibits no significant variation between NPF and non-NPF days, with organics contributing to about 50% of the $PM_{2.5}$, emphasizing the dominance of physical processes. Our observations highlight the critical influence of relative humidity on particle formation, with higher atmospheric liquid water content inhibiting NPF. Additionally, we investigated the simultaneous time variations in PSD and mass composition of $PM_{2.5}$, revealing significant mass composition variations during the first (daytime) and second (night-time) growth. Notably, during the daytime growth of nucleated particles, increases in sulphate and low volatile oxygenated organics suggest the involvement of sulphuric acid and oxidized vapours in early particle growth. However, the unclear relationship between the growth rate and chemical composition reveals the complexity of new particle formation in polluted environments such as Delhi. While $PM_{2.5}$ composition offers insights into growth processes, its relevance to nucleation-mode particles is limited. Thus, this study further emphasizes the need for sub-10 nm PSD and precursor gaseous measurements to seek a better understanding of NPF in a high CS environment in the Global South.

Received 12th August 2024
Accepted 21st October 2024

DOI: 10.1039/d4ea00114a

rsc.li/esatmospheres

Environmental significance

New Particle Formation (NPF) is typically suppressed in polluted urban environments due to the high concentrations of preexisting particles, which act as a condensation sink (CS) for gaseous precursors. However, NPF events are still observed in places such as Delhi. In this study, we combined one year of particle number size distributions and $PM_{2.5}$ chemical composition data to explore the factors influencing NPF in Delhi. Although some studies propose that the chemical composition of particles affects the CS by altering particle hygroscopicity and the contact angle, our findings suggest that chemical composition was not a significant factor. Instead, we found that variations in relative humidity (RH) influenced aerosol liquid water content (ALWC), which played a crucial role in either promoting or inhibiting NPF events. This highlights the variability among different polluted environments, where meteorological conditions, particularly RH, can significantly influence the occurrence of NPF events.

[a]*Department of Chemical Engineering, Indian Institute of Technology Delhi, New Delhi, India. E-mail: vs225@iitd.ac.in*

[b]*Department of Mechanical Engineering, Indian Institute of Technology Delhi, New Delhi, India*

[c]*Centre for Atmospheric Sciences, Indian Institute of Technology Delhi, New Delhi, India. E-mail: shahzadgani@iitd.ac.in*

[d]*Institute of Atmospheric and Earth System Sciences/Physics, University of Helsinki, Finland*

† Electronic supplementary information (ESI) available. See DOI: https://doi.org/10.1039/d4ea00114a

1. Introduction

Delhi, the capital city of India, consistently ranks among the most polluted cities in the world. The concentration of fine particulate matter ($PM_{2.5}$) in Delhi's air often exceeds the World Health Organization's recommended levels throughout the year, posing severe health risks to its residents. While extensive research has been conducted to identify the sources and

mechanisms of pollution in Delhi, the primary focus is either the chemical or physical aspects of source $PM_{2.5}$. Numerous studies in Delhi have focussed on the seasonal variations and source identification of $PM_{2.5}$ mass composition and how these different components contribute to pollution levels in Delhi.[1–5] A few studies have also investigated the seasonal and diel variations of particle number size distribution (PNSD) in Delhi.[6,7] These studies reported significant seasonal variations in the particle number concentration and size distribution, following variations in $PM_{2.5}$ mass concentrations, emphasizing the effect of variations in meteorological conditions and emission sources. However, the observed variation in the particle number and mass concentrations between different seasons was not proportional, indicating that physical processes such as coagulation and condensation sink influence the intricate interplay between the particle number and mass concentrations.

A critical gap remains in understanding the complex interactions between the physical and chemical properties of submicron particles. In particular, new particle formation (NPF), the dominant pathway of gas-to-particle conversion, is defined as the formation of cluster mode particles and their subsequent growth to stable sizes in the atmosphere. New particle formation in Delhi is less understood because NPF is heavily influenced by the concentration of pre-existing aerosol particles.[8–10] High concentrations of pre-existing aerosol particles serve as a condensation sink (CS) for gaseous vapours, potentially leaving fewer vapours available for new particle formation. Even if clusters are formed and grow beyond the critical size and become stable against evaporation, their survival is still primarily determined by coagulation scavenging by existing particles. Consequently, NPF has less significance in contributing to pollution levels in Delhi compared to other factors, leading to less focus and fewer studies on NPF in the city. Despite this, NPF events have been documented in Delhi, especially during the spring and summer, even when CS values are theoretically too high for NPF to occur.[11–15] This paradox suggests that factors beyond simple condensation, such as the physical state, morphology, and chemical composition of particles, play a significant role in the NPF process. These studies have investigated the variation of factors such as the sulphuric acid concentration, CS, and meteorological parameters between NPF and non-NPF days. Although there has been progress in general knowledge, there is still a lack of certainty regarding the extent, variability, and even the direction of the effects of these variables. Factors such as the chemical composition of existing particles can impact the effectiveness of CS by altering properties such as hygroscopicity and the contact angle for heterogeneous nucleation.[16] A recent study in Beijing explored the effect of chemical composition on CS and observed a marked difference in chemical composition between NPF and non-NPF event days for the same CS range.[17] Understanding the role of meteorological and atmospheric variables and the chemical composition of existing particles in the mechanisms of NPF under real atmospheric conditions, particularly in urban environments such as Delhi, remains uncertain.

Furthermore, some studies have used simultaneous chemical composition and PNSD to understand particle growth, but these have predominantly focused on night-time or nocturnal growth. For example, Sarangi *et al.*[12] observed night-time particle growth during the summer, attributing it to high relative humidity (RH) and stable atmospheric conditions that enhance the condensation of vapours. High concentrations of trace gases such as NO_2 and SO_2 and particulates such as SO_4 and NO_3 characterized these growth events. Mishra *et al.*[18] examined nocturnal particle growth during winter, finding that low temperatures and high RH at night drive the rapid condensation of organic vapours from biomass burning. However, the specific species responsible for the formation and growth of the nucleation mode of particles during the daytime have not been investigated.

In this study, we investigated the seasonal variations in particle number concentrations in Delhi, correlating these changes with atmospheric conditions and emission sources. We focused on evaluating the role of CS in NPF and the overall behaviour of particle size distribution (10–1000 nm), identifying CS as a primary factor influencing NPF. We examined the availability and impact of chemical precursors, such as sulfuric acid (estimated through proxy), ammonia, and SO_2, on NPF across different seasons, determining their significance relative to physical processes. Furthermore, we investigated the chemical composition of existing particles, analysing how variations in chemical composition affect the CS and, consequently, NPF processes. In tandem, we assessed the influence of RH and atmospheric liquid water content (ALWC) on NPF, particularly regarding the inhibitory effects of higher ALWC. Additionally, we analysed temporal variations in particle size distribution and the $PM_{2.5}$ mass concentration to indirectly identify the broader sources of vapours that may play a role during different stages of particle growth. The enhancement in sulphate and low volatile oxygenated organic fractions during daytime growth suggests the probable role of sulphuric acid and oxygenated low volatile organics in the initial daytime growth of newly formed particles. By exploring the relationship between particle growth rates and chemical composition, we aimed to unravel the complexities of NPF in Delhi.

2. Materials and methodology

2.1 Instrumentation and data acquisition

The sampling was conducted inside the campus of the Indian Institute of Technology Delhi (IITD) in the southern part of Delhi. This site has been acknowledged as an urban background representative and utilized as a sampling location in various previous studies.[3–5,19,20] More details about the sampling site are given in S1.† The sampling period comprised two winters: January 2022 to mid-February 2022 and December 2022 to mid-January 2023, spring: mid-February to March 2022, summer: April to June 2022, and autumn or post-monsoon: mid-October to November 2022. A scanning Mobility Particle Sizer (SMPS) (GRIMM SMPS + C 5416) was deployed to measure the submicron size distribution ranging from 10 to 1000 nm at a 4-minute resolution. An SMPS has a neutralizer, an extended

differential mobility analyser (DMA), and a butanol-based condensation particle counter (CPC). The real-time measurements of non-refractory ($NR\text{-}PM_{2.5}$) chemical components (organics, SO_4^{2-}, NO_3^-, NH_4^+, and Cl^-) were obtained *in situ* using an Aerosol Chemical Speciation Monitor (ACSM) at a time resolution of 10 minutes. An aethalometer (AE33) was used to measure refractory black carbon (BC). The details about instrument operation and calibrations are provided in ESI Section S2.† The measured $PM_{2.5}$ concentrations (comprising $NR\text{-}PM_{2.5}$ and BC) agreed well with the mass concentrations of PM_1 calculated from particle number size distributions (PNSDs). This indicates that the instruments used for these measurements operated reliably and consistently. More details about the density used and mass closure are given in ESI Section S3.†

The measurements of concentrations of $PM_{2.5}$ and gases such as CO, NO, NO_x, SO_2, NH_3, and O_3 were sourced from the closest CPCB station – the Pollution Control Committee (DPCC) monitoring station situated at RK Puram approximately within a 2-kilometre radius of the sampling site. Temperature, relative humidity (RH), wind speed (WS), and wind direction (WD) were measured at the sampling site.

Aerosol liquid water content (ALWC) was estimated using the thermodynamic model ISORROPIA II, and the details are given in ESI Section S4.† Source apportionment of organics measured from ACSM was performed using positive matrix factorization and is explained in ESI Section S5.†

Additionally, planetary boundary layer height (PBLH) data were obtained from the National Aeronautics and furthermore, data on planetary boundary layer height (PBLH) are sourced from the National Aeronautics and Space Administration (NASA) meteorological reanalysis dataset, MERRA2, which is accessible through the NASA Goddard Earth Sciences Data and Information Services Centre (GES DISC) website (**https://gmao.gsfc.nasa.gov/reanalysis/MERRA-2/**). The global radiation data for Delhi was obtained from the European Centre for Medium-Range Weather Forecasts ECMWF-ERA5 reanalysis dataset. All times mentioned in this study are local (LT) and recorded in Indian Standard Time (IST), corresponding to GMT + 5:30.

2.2 Size-resolved particle concentrations

Wide-range particle size measurements have been grouped into five modes: (a) cluster mode, (b) nucleation mode, (c) Aitken mode, (d) accumulation mode, and (e) coarse mode. Cluster mode represents the particles of the smallest size range (1–3 nm), which is not covered in this study due to instrument limitations. Nucleation is the next mode, which has been described as particles with sizes below 15 nm, 20 nm, 25 nm, or 30 nm.[6,21–23] In this study, we have used the most common classification of particle size distribution into three modes: nucleation (10–25 nm), Aitken (25–100 nm), and accumulation (100–1000 nm). The nucleation and Aitken modes constitute the ultrafine mode (10–100 nm). It is important to note that the minimum detection limit in our instrument is 10.55 nm. Because PNSD follows a log-normal distribution, a significant number of nucleation mode particles below the size of 10.55 nm are not measured in this study; the actual PN concentration of nucleation mode will be higher than that reported.

2.3 NPF identification

We plotted the particle size distribution with time as a heatmap plot, with D_p on the *y*-axis, time on the *x*-axis, and normalized particle concentration $\left(\frac{dN}{d\log D_p}\right)$, represented as a function of colour intensity on the heatmap. To identify NPF events, we used the following criteria given by Dal Maso *et al.*[24] and Kulmala *et al.*[25]

(1) First, a sudden burst or high concentration of nucleation mode particles (<25 nm) should be observed at any time and persist for several hours. The time at which burst, or onset occurs usually marks the start of the NPF event.

(2) This onset of the high concentration of nucleation mode particles should show subsequent growth to larger sizes, and the growth should persist for more than 2 hours.

In addition to these two features, Delhi being a polluted city with the continuous influence of traffic and other primary emissions, we plotted temporal variation of primary species, such as BC, NO_x and CO, to exclude primary emissions as the source of nucleation mode of particles.[26,27] We also examined the temporal variations of various PNC modes, observing that a simultaneous variation in the concentration of all modes may indicate shifts in meteorological conditions or emissions. Furthermore, when the particle growth rates in an NPF event can be accurately estimated from the temporal evolution of PNSDs, we categorized it as a 'Type I' event; otherwise, it is categorized as a Type II event. More details are provided in ESI Section S6.†

We acknowledge that the absence of sub-10 nm PNSD data limits our ability to fully distinguish nucleation events from the growth of primary emissions. Future studies should incorporate sub-10 nm measurements and additional precursor gases to provide a clearer distinction between these processes.

2.4 Condensation sink (CS)

Condensation sink (CS) quantifies the rate at which vapour molecules condense onto existing aerosols. CS is calculated using the following relationship:[28]

$$CS = 2\pi D_{vap} \sum \beta_M D_p N \quad (1)$$

where N and D_p represent the number concentration and diameter of the particles, respectively, and D_{vap} is the diffusion coefficient of condensing vapour. We used the following relationship to determine D_{vap}:[29–31]

$$D_{vap} = 0.001 \times T^{1.75} \frac{\sqrt{M_{air}^{-1} + M_{vap}^{-1}}}{P\left(D_{x,air}^{\frac{1}{3}} + D_{x,vap}^{\frac{1}{3}}\right)^2} \quad (2)$$

for $T = 293$ K and $P = 1$ atm. ${D_{x,\mathrm{air}}}^{1/3}$ and ${D_{x,\mathrm{vap}}}^{1/3}$ are the effective sizes of the air and the vapour molecules, respectively, and M_{air} and M_{vap} are the molar masses for air and diffusing vapours, respectively.

The Fuchs–Sutugin correction factor (β_{M}), also known as the transitional correction factor, is computed according to the following formula:[32]

$$\beta_{\mathrm{M}} = \frac{1 + K_{\mathrm{n}}}{1 + \left(\frac{4}{3\alpha} + 0.377\right)K_{\mathrm{n}} + \frac{4}{3\alpha}{K_{\mathrm{n}}}^2} \quad (3)$$

where K_{n} is the Knudsen number, which is calculated as:

$$K_{\mathrm{n}} = 2\lambda_{\mathrm{m}}/D_{\mathrm{p}} \quad (4)$$

where λ_{m} is the mean free path of the vapours and α is the mass accommodation coefficient that describes the probability that a vapor molecule or cluster will stick to a particle upon collision.

While calculating the CS, it is usually assumed that the α is equal to one, and sulfuric acid is typically considered the condensing vapor due to its low vapor pressure under typical atmospheric conditions. Additionally, evaporation is often considered negligible, making the effective condensation sink ($\mathrm{CS_{eff}}$) equal to the CS, and the CS represents the total vapor loss rate. Furthermore, the CS will depend on the properties of condensing vapour, such as molecular mass. Suppose the properties of the condensing vapor for CS calculation are assumed to be those of sulfuric acid. In that case, the loss rate of the vapor will be overestimated in the case of high molecular mass organic vapours. The uncertainties arising from these assumptions while estimating CS were discussed by Tuovinen *et al.*[33]

2.5 Growth rate

The apparent growth rate (GR) of new particles was calculated using the formula:

$$\mathrm{GR} = \frac{\Delta D_{\mathrm{p}}}{\Delta t} \quad (5)$$

where ΔD_{p} represents the increase in the geometric mean diameter of the nucleation mode. Δt is the duration for the growth of new particles (from the start to the end of an NPF event) (Fig. S8†).

In analysing atmospheric particle size distribution, multiple log-normal distribution functions were employed to fit the PNSD data measurements from SMPS.[34] Furthermore, we only measured particles larger than 10 nm, potentially underestimating nucleation mode particles. Our study lacks data on sub-10 nm, which can lead to uncertainties in growth rates. Including the full nucleation mode range and addressing uncertainties in growth rates can enhance our understanding of NPF.

2.6 Apparent (J_{10}) and real nucleation ($J_{1.5}$) rates

The critical cluster size is about 1.5 nm.[35–37] The real nucleation rate ($J_{1.5}$) was estimated from J_{10} values using the method by Kerminen and Kulmala.[38]

$$J_{1.5} = J_{10} \exp\left[\frac{\eta}{d_{10}} - \frac{\eta}{d_{1.5}}\right] \quad (6)$$

where the factor η is given by

$$\eta = \frac{\gamma \mathrm{CS}'}{\mathrm{GR}} \quad (7)$$

where γ is assumed constant at 0.23 $\mathrm{m^2\ nm^2\ h^{-1}}$ and CS′ is condensation sink in the units of $\mathrm{m^{-2}}$. γ may vary with the shape of the initial particle size distribution, the initial size and density of the nuclei, and the surrounding pressure and temperature.[38]

The apparent formation rate (J_{10}) was estimated using the method described by Kulmala *et al.*[25] and has been explained in ESI Section S7.† The estimation of nucleation rate $J_{1.5}$ based on eqn (6) has significant uncertainties. The assumption of constant growth rates from 1.5 to 25 nm (*i.e.*, $\mathrm{GR} = \mathrm{GR_{1.5–10}} = \mathrm{GR_{10–25}}$) introduces uncertainties.[39–41] The growth rate may be more pronounced in smaller particles, while different condensable vapours, such as organics, become relevant in larger particles due to the Kelvin effect.[8] Additionally, neglecting intermodal coagulation could lead to an underestimation of $J_{1.5}$. The assumptions and uncertainties related to this method were discussed in detail by Kerminen and Kulmala.[38]

2.7 H_2SO_4 proxy

Sulphuric acid is widely recognized as the predominant nucleating agent due to its low vapor pressure under typical atmospheric conditions and its tendency to interact with various crucial atmospheric compounds through hydrogen bonding. Our study lacks direct measurements of the concentration of sulphuric acid in air. In order to determine the atmospheric concentration of sulphuric acid (in molecules per $\mathrm{cm^3}$) while its production and loss rates are in the steady state, we employ the following proxy relationship:[42]

$$\mathrm{H_2SO_4\ _{proxy}} = -\frac{\mathrm{CS}}{2k_3} + \left[\left(\frac{\mathrm{CS}}{2k_3}\right)^2 + \frac{[\mathrm{SO_2}]}{k_3}(k_1\mathrm{GlobRad} + k_2[\mathrm{O_3}]\mathrm{alkene}])\right]^{1/2} \quad (8)$$

GlodRad: global radiation ($\mathrm{W\ m^{-2}}$) correlates well with ultraviolet B (UVB) radiation,[43–45] which is a good proxy for the OH concentration.[46,47] CS: condensation sink, which represents the rate of loss of H_2SO_4 molecules due to existing particles. k_1: the coefficient for H_2SO_4 production from the reaction between SO_2 and OH radicals during daytime. k_2: the coefficient for H_2SO_4 production from the ozonolysis of alkenes, predominantly at night. k_3: the clustering coefficient, representing the rate of H_2SO_4 loss due to cluster formation. SO_2: the concentration of sulphur dioxide (molecules per $\mathrm{cm^3}$).

In our case, we do not have the alkene concentration, and oxidation of SO_2 through OH is the dominant pathway during daytime, so we only estimate the daytime H_2SO_4 concentration. Furthermore, we used the previously determined values for k_1,

k_2, and k_3 from Beijing, which are 2.0×10^{-8}, 1.5×10^{-29}, and 7.0×10^{-9}, respectively.[42] More details and other proxies are given in ESI Section S7.†

3. Results and discussion

3.1 Aerosol PNC characterization

3.1.1 Seasonal variation. Seasonal variation in emission sources, meteorological conditions, and atmospheric processes leads to subsequent variations in particle size characteristics. This section discusses the seasonal variation of the number concentration of total and size segregated modes (nucleation, Aitken, and accumulation). The average number of total and different modes in different seasons are given in Table S1,† and the descriptive analysis is shown in Fig. 1. The average total particle number concentration during the study period was 3.48×10^4 cm^{-3}. The highest concentration of total particles was observed in the winter season, with an average concentration of 4.11×10^4 cm^{-3}. In contrast, the lowest concentration was observed in summer, with an average concentration of 2.53×10^4 cm^{-3}. The post-monsoon and spring seasons marked average concentrations of 3.92×10^4 cm^{-3} and 3.57×10^4 cm^{-3}, respectively. The variation in total PN levels across seasons follows the seasonal variation of the $PM_{2.5}$ mass concentration, though not in a direct proportion (Fig. S9†). For instance, while the PN levels in winter are less than two times those in summer, the $PM_{2.5}$ levels in winter are more than three times the summer levels.

The variation in the number and mass concentration across different seasons can be attributed to the difference in emission sources, meteorological parameters and atmospheric processes that govern them. Fig. S10† shows the diel variation of meteorological parameters during different seasons. As evident from these plots, seasonal variations of the particle number concentration closely follow the variations in meteorological parameters such as PBLH, RH, T, and WS. Low PBLH, WS, and T during winter make conditions unfavourable for the dispersion of pollutants. The average number of concentrations reported in this study is similar to the earlier reported observations,[7] covering winter, summer, and post-monsoon (autumn) periods. However, the average PN concentration levels reported in a previous study[6] based on measurements from 2017–1018 during winter (52.5×10^4 cm^{-3}), spring (49×10^4 cm^{-3}), summer (4.34×10^4 cm^{-3}), and autumn (3.8×10^4 cm^{-3}) were higher. This variation can be potentially explained by the different periods and emissions, which is also evident from the average mass concentrations observed in their campaign. This shows that although the PN and PM levels in Delhi are still

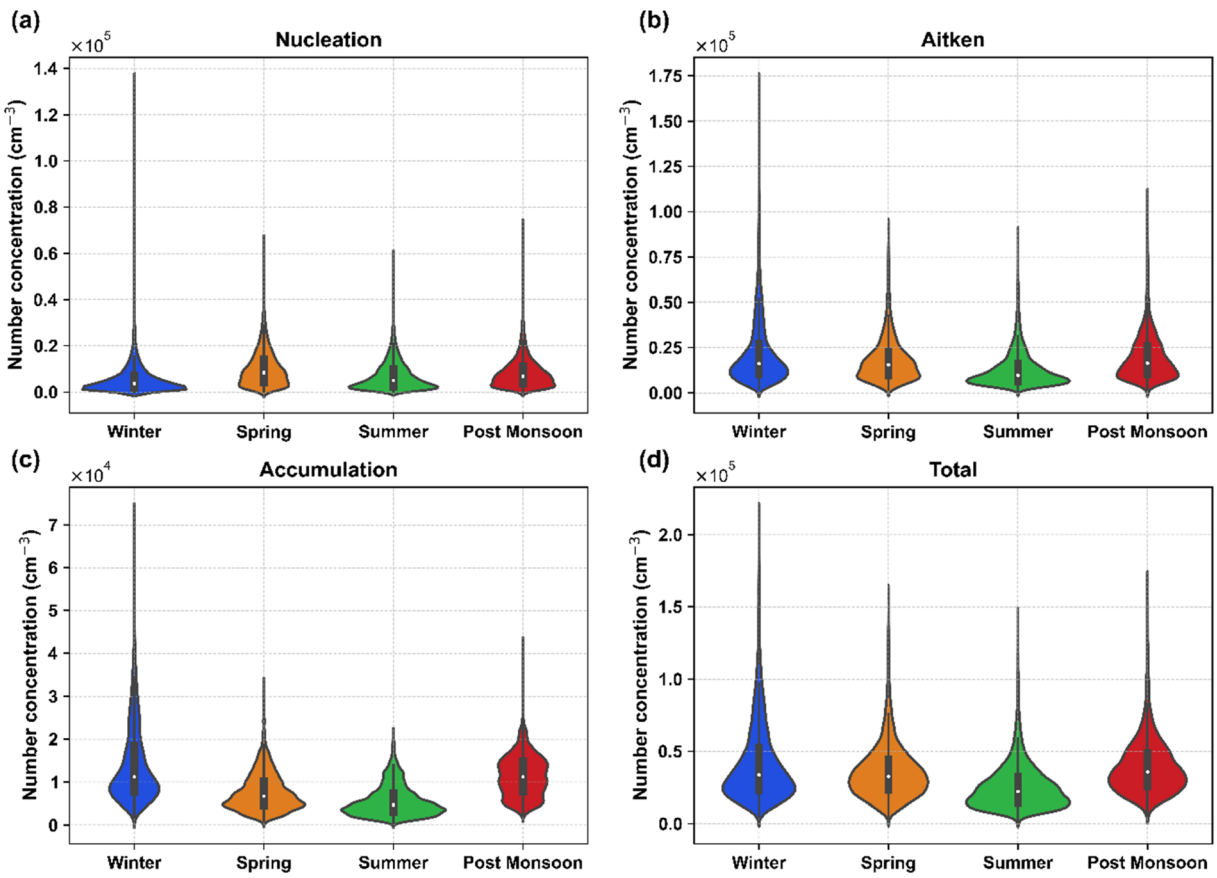

Fig. 1 Seasonal variation in average particle number concentrations of (a) nucleation mode, (b) Aitken mode, (c) accumulation mode, and (d) total, depicted using violin plots. These plots display the distribution and density of concentrations with the central white dot inside each box indicating the median value. The data reveal that total particle number concentration peaks during colder seasons (winter and post-monsoon), while the nucleation mode is more prevalent in warmer periods and the accumulation mode is more pronounced during colder periods.

higher in recent years, there has been a decline in the PN and PM mass concentrations. On comparing these observations with other global megacities, the number concentration reported in Delhi is significantly higher than that in Chinese cities such as Beijing, which also experience a high mass concentration of particulate matter.[48]

In terms of modes, the Aitken mode was the dominant contributor across all seasons, contributing around 50% to the total PNC. Regarding concentrations, Aitken mode was highest during the winter season with an average concentration of 2.13 $\times$ 10^4 cm^{-3}. Post-monsoon also had a similar concentration to winter, while the summer season had the lowest concentration of Aitken mode, almost 50% lower than that in winter (1.28 $\times$ 10^4 cm^{-3}). Previous studies from different urban regions have attributed vehicular emissions, especially Aitken mode, to be the dominant source of submicron PN concentration.[48–52] The similar diel variations shown by Aitken mode and NO_x (Fig. S11†) further suggest that traffic is a dominant source of Aitken mode particles. Other sources contributing to the Aitken mode include biomass burning, cooking, solid waste burning, industrial emissions, and construction activities.[53–56] This shows that the traffic sector is the dominant contributor of particles in Delhi, which has also been observed in other cities, especially near road sites.[57,58]

The concentration of nucleation mode particles was higher in warmer periods than in colder seasons, which was also observed in the previous studies.[7,59] In our study, spring had the highest particle number concentration of nucleation mode (1.01 $\times$ 10^4 cm^{-3}), followed by post-monsoon and summer. Winter had the lowest concentration of nucleation mode particles, potentially due to the high loading of Aitken and accumulation mode particles, which scavenge smaller nucleation mode particles and condensable vapours, thereby inhibiting new particle formation. We observed a lower nucleation number concentration in the summer than in the highly polluted post-monsoon season. Still, in terms of fractions, nucleation mode contributed 27% of the total PN concentration during summer as compared to 20% during post-monsoon.

Although a more significant fraction of particles was in ultrafine mode (<100 nm) throughout each season, a considerable portion was in accumulation mode. The winter season has the highest concentration (1.42 $\times$ 10^4 cm^{-3}) of accumulation mode particles, followed by post-monsoon (1.15 $\times$ 10^4 cm^{-3}). The lowest concentration of accumulation mode was observed in the summer and spring seasons, with concentrations of (5.62 $\times$ 10^3 cm^{-3}) and (7.65 $\times$ 10^3 cm^{-3}), respectively. The accumulation mode contributed to about 35% of the total PN concentration and more than 96% of the total PM_1 mass concentration during winter. In comparison, the contribution to the total PN concentration reduced to 22% during summer, and the contribution to the PM_1 mass concentration remained at 95%. Variation of accumulation mode PN concentrations follows the seasonal variation of $PM_{2.5}$ mass concentrations, which is expected as almost all the mass of $PM_{2.5}$ is contributed by this mode. On average, the accumulation mode contributed about 28% of total PNC during the entire study period, which is significantly higher compared to relatively less polluted European and Western regions but consistent with the earlier studies in Delhi and other South Asian regions.[6,7,23]

3.1.2 Diel variations. Diel variations of PN concentrations of total and different modes during different seasons are shown in Fig. 2. Total and individual mode PN concentrations varied through the day during each season, indicating that the PNSD is influenced by the relative strength of sources, meteorological parameters, and atmospheric processes throughout the day.

During winter, the average hourly total PN concentration varied from 2.8 $\times$ 10^3 cm^{-3} during the afternoon at around 15:00 LT to 8.0 $\times$ 10^3 cm^{-3} during evening hours at around 20:00 LT. The post-monsoon hourly averaged total PN concentration varied from a minimum value of 2.2 $\times$ 10^3 cm^{-3} at 14:00 LT to 5.8 $\times$ 10^3 cm^{-3} at 20:00 LT. Spring and summer diel plots of total PN concentration also showed a similar time variation, with minimum values at 15:00 LT and maximum values at 20:00 and 21:00 LT in the evening. The high PN concentration during morning and evening rush hours suggests that traffic is Delhi's dominant source of PN concentration. This is further validated by the diel plots of NO_x and CO, which also peak during these hours (Fig. S10†). During spring and summer, we also observed small peaks in the afternoon at around 12:00 LT and 13:00 LT, respectively. High photochemical activity and low pollution levels during summer and spring, mainly during the daytime, make the formation and survival of new particles feasible.

Aitken mode followed a similar diel variation to total PN across each season, with two peaks at rush hours. This again indicates that Aitken is the dominant mode of particles during each season. Nucleation mode showed different diel variations across different seasons. During winter and post-monsoon, nucleation mode showed two peaks, one each in the morning and evening, resembling the Aitken mode diel peaks, indicating traffic emissions as the dominant contributor of nucleation mode during rush hours. However, during warmer seasons, nucleation mode showed an afternoon peak, which can be attributed to the NPF events associated with low coagulation and condensation sinks during these seasons.

Similar observations can be made from the seasonal heatmap plots shown in Fig. S12.† Nucleation mode particles typically form during the daytime, followed by subsequent growth throughout the day or part of the day. The formation, survival, and growth of these nucleated particles are strongly favoured by the lower concentration of pre-existing particles that otherwise act as sinks for smaller particles and condensable vapours. Other factors include the concentration of sulphuric acid and other highly oxidized and low-volatility organic vapours, which form due to photochemical oxidation, the amount of solar radiation, RH, T, and atmospheric mixing.[60] The number concentration of this nucleation mode decreased towards the night hours, which can be due to the absence of nucleation processes, condensational growth to larger particles, and coagulation onto the existing particles.[6]

3.2 New particle formation

During the sampling period, we observed NPF on 50 days out of 204 days, which gives a frequency of about 25%. Most of the

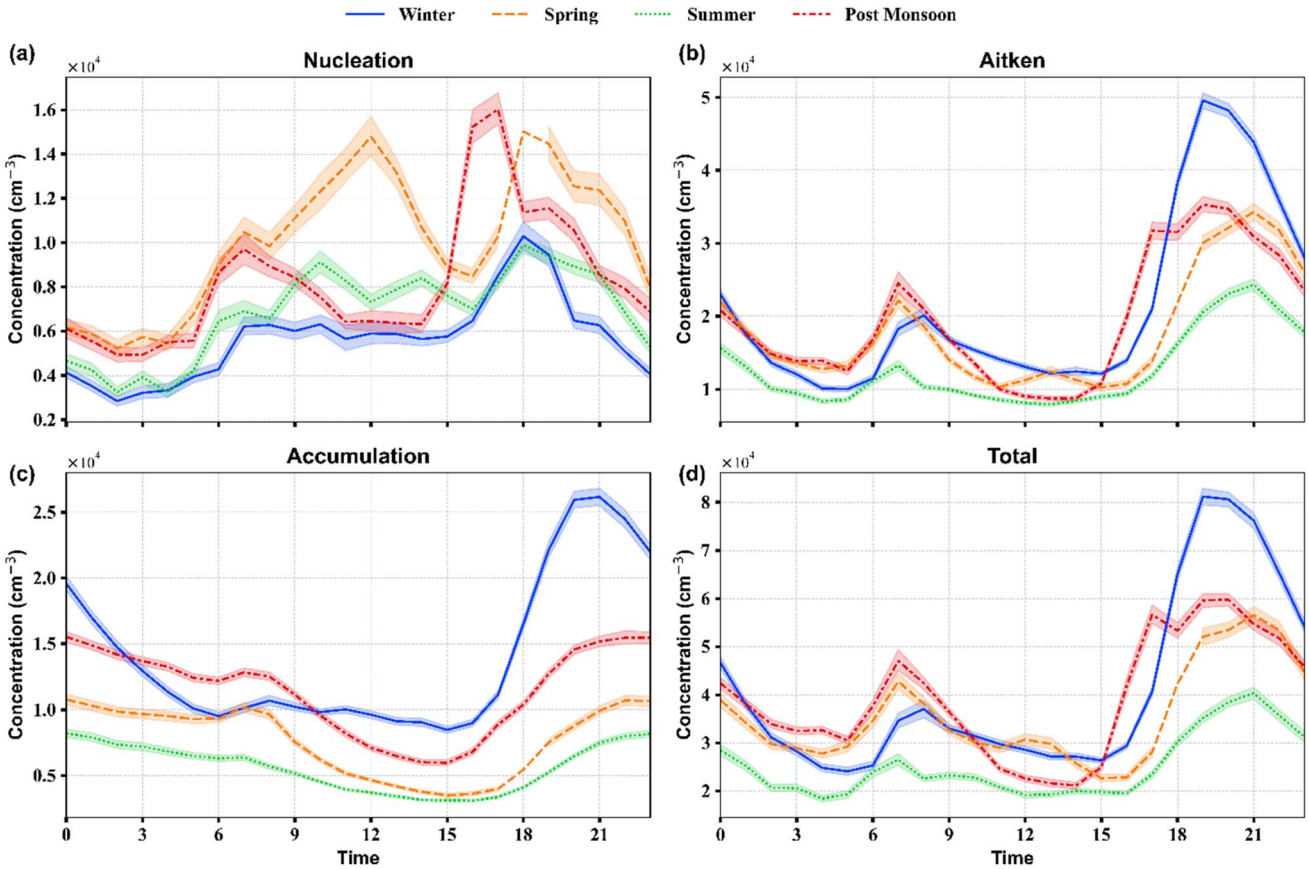

Fig. 2 Average diel variation in particle number concentrations for (a) nucleation mode, (b) Aitken mode, (c) accumulation mode, and (d) total for different seasons.

observed NPF events were confined to spring and summer seasons. Among the NPF events, the days that met all the conditions mentioned in Section 2.3 were classified as Type I events (Fig. 3a and b), represented the typical regional scale NPF events and had a frequency of 18%. The events that did not last for a long time or did not show the typical banana-type pattern were classified as Type II NPF events (Fig. 3c). The days that did not show any feature of either nucleation or growth were considered non-NPF events (Fig. 3d). The corresponding diel variations of mass concentrations of NO_x and number concentrations of different modes are given in Fig. S5 and S6.† Earlier studies in Delhi reported different NPF frequencies (30–53%)[11–15] compared to the present observations. However, these studies were mostly limited to shorter durations (1–3 months), mostly confined to warmer seasons, and instruments with different minimum cutoff sizes were used. Our study agreed with a long-term study by Jose *et al.*,[61] which reported an NPF frequency of 17% for well-defined NPF events, comparable to our observation. The NPF frequency was lower than that in other polluted urban sites globally, such as Beijing (40%).[17,62,63] In particular, the NPF events are observed during each season at these sites instead of being confined to warmer seasons only.

The mean GR during our study period was 5.72 nm h^{-1} and ranged from 3.2–10 nm h^{-1}. The GRs observed in our study agree with the earlier observations recorded in different urban cities of India, such as Pune (6.5 ± 1.2 nm h^{-1}) and Kanpur (8.7 ± 3.2 nm h^{-1}),[64] and for coastal semi-urban area Thumba (7.35 ± 2.93 nm h^{-1}).[65] The average growth rate in our study was similar to the earlier observed average growth rate of 5.86 ± 1.44 nm h^{-1},[13] in Delhi. Higher GRs of 11.6–18.1 nm h^{-1} and 15–30 nm h^{-1} have also been reported over Delhi.[11,14] However, these high GRs were observed when pollutant/condensable vapor concentrations were still elevated during the colder period.

In addition to the first type of growth of these newly formed particles during the daytime, a second type of growth was observed starting from evening and continuing until midnight. This second type of growth has also been reported in the previous studies during all seasons in Delhi.[7,59] The freshly emitted primary particles emitted in the nucleation size range during traffic rush hours, alongside the previously grown particles, undergo rapid growth from evening until midnight. Previous studies have attributed this rapid growth to either condensation or coagulation processes which may be happening simultaneously during these hours. Higher concentrations of accumulation and Aitken particles resulting from increased emissions and reduced mixed layer lead to a higher coagulation sink of the freshly emitted particles.[6] This is evident from rapid reduction in nucleation and Aitken mode PN concentrations after the late evening hours but

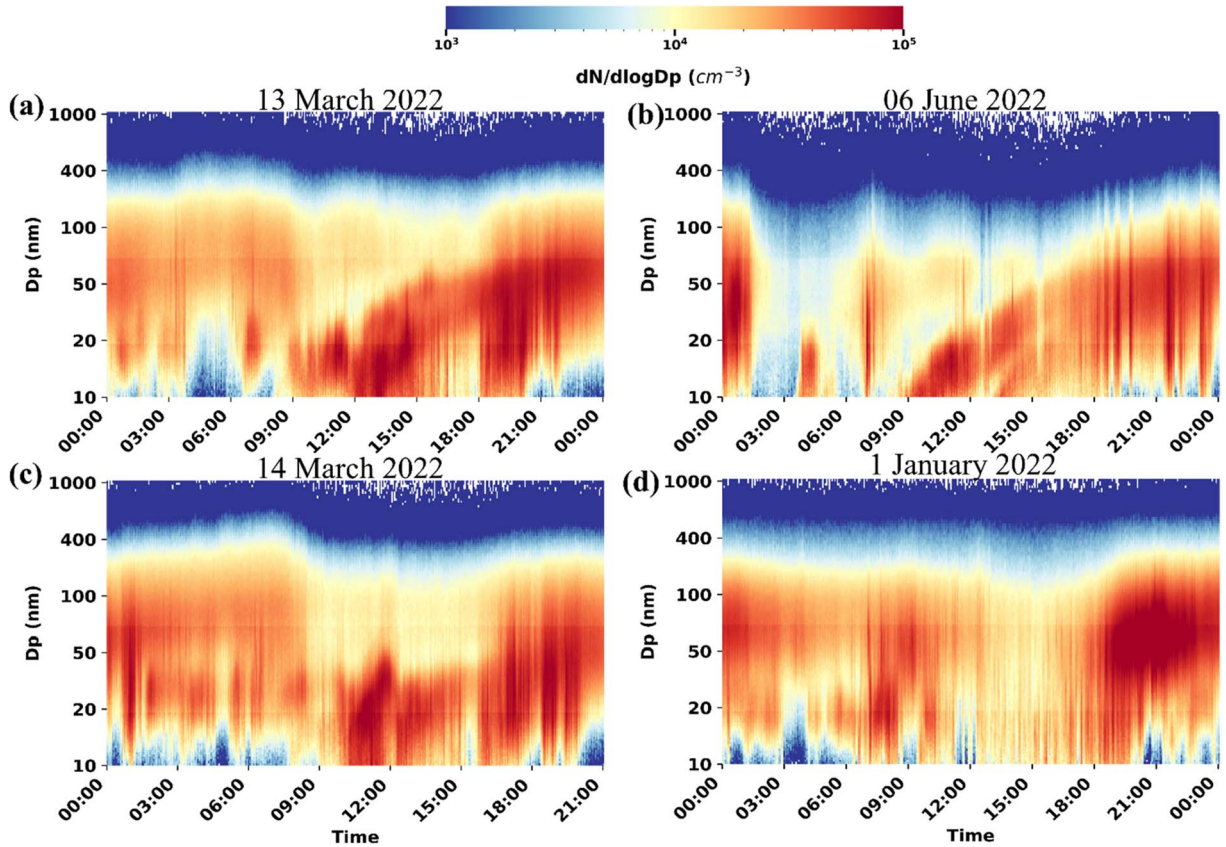

Fig. 3 (a) and (b) Typical Type I NPF events. A nucleation mode appears at around 11 AM and undergoes condensational growth. This can also be observed from the temporal variation of nucleation mode of particles which started to increase at 11 AM. (c) A type II NPF event; no prolonged growth and hence a typical banana could not be observed. (d) A non-NPF event with no feature of NPF identification observed.

accumulation and $PM_{2.5}$ mass concentration remaining unchanged or showing relatively lower reduction (Fig. 2). However, the simultaneous decrease in T and increase in RH leads to the condensation of condensable vapours such as emissions from biomass.[12,18] Changes in chemical composition associated with the growth hours support this argument. Furthermore, previous studies have shown that particles with more than 50 nm size substantially impact the development of cloud condensation nuclei (CCN), while particles larger than 100 nm are categorized as haze particles.[66–69] Our observations indicate that the maximum diameter of these newly formed particles ranges between 30 and 100 nm. This implies that Delhi, as an urban region, is likely to face more substantial consequences from haze and climate change because of the high concentration of vapours that promote the growth of newly formed particles.

3.3 CS and new particle formation events

NPF is a complex process affected by various parameters such as pollutant concentrations, meteorological parameters, types of pollutants, *etc.*[8,70–74] To understand the factors governing NPF in Delhi, the concentration of gaseous and particulate pollutants is studied alongside physical (CS) and meteorological parameters (RH, T, solar radiation, and WS). We can obtain clues about the species and factors governing NPF by comparing the abovementioned parameters between observed NPF and non-NPF days. Although the absence of direct measurements of key precursor vapours along with the lack of cluster mode particle size distribution (sub-3 nm) limits our ability to fully understand the early stages of particle nucleation, our study seeks to offer valuable insights into the factors that govern NPF under Delhi's atmospheric conditions.

In polluted environments with a high condensation sink such as Delhi, homogeneous nucleation would appear improbable, and there is competition over whether the vapours will condense on pre-existing particle surfaces or participate in new particle formation.[39,75,76] The condensable vapours and initially formed clusters are inclined to adhere to pre-existing surfaces instead of initiating self-nucleation to form new particles. High concentrations of already existing (pre-existing) particles in the atmosphere, mainly typical in highly polluted environments such as Delhi, act as a sink for the condensable vapours and have been observed to hinder the NPF processes.[15,71,73,77–81] Furthermore, the high concentration of existing particles will lead to coagulation scavenging of the newly formed clusters or initial particles before they can grow to atmospherically relevant sizes, thereby inhibiting NPF. The measure of this tendency of existing particles can be roughly given by the $PM_{2.5}$ mass concentration or, in a better way,

estimating the condensation and coagulation sinks from PNSD. Earlier studies conducted in Delhi have shown that NPF events are observed during the spring and summer seasons when the average $PM_{2.5}$ concentrations are relatively lower.[7,13,61,80] The study observed a consistent pattern of seasonal variation in $PM_{2.5}$ mass concentrations, with the lowest averages recorded during summer and spring and higher concentrations observed during post-monsoon and winter seasons. During our one-year study, the hourly average mass concentration of $PM_{2.5}$ varied from 4 to 996 μg m^{-3}, with an average mass concentration of 107 μg m^{-3}, which is consistent with the earlier reported average $PM_{2.5}$ concentration in Delhi (Table S3†). As expected, CS followed the $PM_{2.5}$ and ranged from 0.004 to 0.8 s^{-1}. During our observations, NPF occurred from 10:00 LT to 16:00 LT, so we averaged the CS during the daytime hours (10:00–16:00 LT), represented as CS in the following discussion. This timeframe is known to encompass the majority of NPF occurrences and their subsequent development. Furthermore, this approach minimizes the impact of morning and evening rush hours at the roadside sites. It focuses only on the period when the rate of particle formation is most significant for NPF events.

Fig. 4a presents the daytime mean $PM_{2.5}$ *versus* CS variation, distinguishing between NPF and non-NPF days. Only two data points fell below CS values of 0.01 s^{-1}, with a corresponding average $PM_{2.5}$ mass concentration of 10 μg m^{-3}, a level typically seen in the upper 75th quartile in clean regions.[82,83] This observation highlights the persistent presence of pollutants throughout all days analysed, emphasizing the severity of pollution in the region. High CS appears to be a primary governing factor for the non-occurrence of frequent NPF events in Delhi. As shown in the CS *vs.* $PM_{2.5}$ plot (Fig. 4a), NPF occurred in Delhi when CS was below 0.06 s^{-1}, corresponding to $PM_{2.5}$ levels of 80 μg m^{-3}. Thus, a CS of approximately 0.06 s^{-1} appears to be the threshold for NPF occurrence in Delhi during our observation period. Most data points above a CS of 0.06 s^{-1} fall in the colder seasons, which align with higher $PM_{2.5}$ mass concentrations (Fig. S8†). The highest CS values for which NPF events have been observed across different regions are summarized in Table S4.† In Delhi, the CS threshold for NPF is around 0.06 s^{-1}, similar to other polluted cities such as Beijing (0.04 to 0.06 s^{-1}) and Shanghai (up to 0.1 s^{-1}). Cleaner regions, such as Helsinki, have lower thresholds (0.01 to 0.03 s^{-1}), where NPF is driven more by the concentration of precursor vapours and other parameters than by CS. In remote areas such as the Western Himalaya (0.0058 s^{-1}) and Arctic (0.001 to 0.002 s^{-1}), the influence of CS on NPF is further minimal. Furthermore, in less polluted and cleaner regions, the CS difference between NPF and non-NPF event days is often less significant, with similar CS values observed on both types of days, indicating that CS is not the decisive factor in these regions.[84–87] The variability in CS thresholds across regions reflects the diverse atmospheric conditions and the interplay between pre-existing particle concentrations and precursor vapor availability and composition.

NPF in polluted environments persists despite elevated CS values, likely due to the abundant availability of precursor vapours such as sulfuric acid, ammonia, and volatile organic compounds that drive nucleation. The presence of strong nucleating agents, such as amines, coupled with rapid cluster growth, enhances the survival and growth of particles. Moreover, reduced scavenging efficiency of molecular clusters may help reconcile the apparent discrepancy between high CS values and observed NPF events in these environments.[10] However, in our case, the lack of measurements of NPF precursors limits our ability to explain these processes in detail.

During winter and post-monsoon seasons in Delhi, the combination of high CS and coagulation sink poses significant challenges for new particle formation. Additionally, the aerosols in Delhi exhibit high hygroscopicity, as noted in previous studies,[3,88,89] leading to enhanced growth in size and ALWC. This amplified particle growth further increases CS beyond estimated dry CS levels, which leads to scavenging of condensable vapours and any newly formed clusters onto these grown particles. Furthermore, the hygroscopic nature of

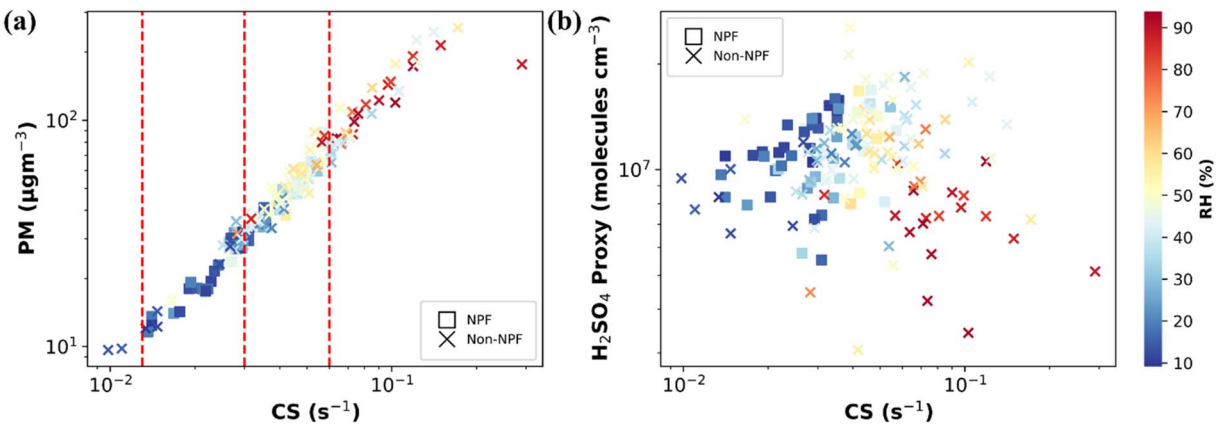

Fig. 4 (a) Average daily variation of $PM_{2.5}$ (μg m^{-3}) *vs.* CS (s^{-1}) marked and coloured as the function of RH and (b) average daily variation in the H_2SO_4 proxy concentration (molecules cm^{-3}). Each data point is the average of the variable from 10:00 to 16:00 LT. No NPF event was observed when average daytime CS was above 0.06 (s^{-1}), most of which were observed in colder post-monsoon and winter periods. H_2SO_4 was also lower during these days. The figure highlights that NPF events were absent on some days despite higher H_2SO_4 and lower CS values. Vertical dashed red lines are included to delineate different CS regions.

condensable vapours such as sulphuric acid and oxidized organic molecules results in their uptake into the liquid water content of aerosol particles, providing an additional sink for these vapours. Consequently, no NPF events are observed during these seasons. In contrast, Delhi's summer and spring seasons are relatively cleaner, with lower CS during the daytime. Despite this, the CS remains higher compared to other cleaner regions globally. However, NPF events are still observed due to Delhi's high concentration of condensable vapours.

The availability of condensable vapours, particularly sulfuric acid, plays a pivotal role in NPF processes. Studies worldwide have shown that sulphuric acid is the precursor of new particle formation.[8,70–75,90–93] Sulfuric acid is widely recognized as the predominant nucleating agent due to its tendency to maintain a low vapor pressure under typical atmospheric conditions.[37,70,94–96] Moreover, it readily engages in hydrogen bonding interactions with various crucial atmospheric compounds such as water, basic species and organic acids.[70] This capacity to establish hydrogen bonds makes sulfuric acid exceptionally suitable for participating in nucleation processes. Specifically, the initial clusters preceding nucleation exhibit a distinct state separate from the liquid phase, and the primary step of nucleation, namely the formation of dimers, is primarily propelled by hydrogen bonding. This has been confirmed by the observed positive correlation between formation rates of newly formed particles and the sulphuric acid concentration.[37,39,72,90,96–98] However, direct measurements of sulphuric acid concentration were unavailable in our study. Instead, we utilized a sulfuric acid proxy to compare concentrations between NPF and non-NPF days, providing insight into the role of sulfuric acid in facilitating NPF events. Fig. 4b illustrates the variation of daytime average sulphuric acid with CS on NPF and non-NPF days. Generally, the frequency of NPF events decreases with increasing CS, with NPF events in higher CS regimes associated with elevated H_2SO_4 concentrations. However, there is no clear distinction between NPF and non-NPF events as a function of H_2SO_4 concentration. This lack of clarity may be attributed to the role of other vapours such as amines or oxygenated organics and other predictive variables, including relative humidity, the presence of other condensable vapours, CS effectiveness, and prevailing meteorological conditions, which may also play significant roles in influencing NPF occurrences.

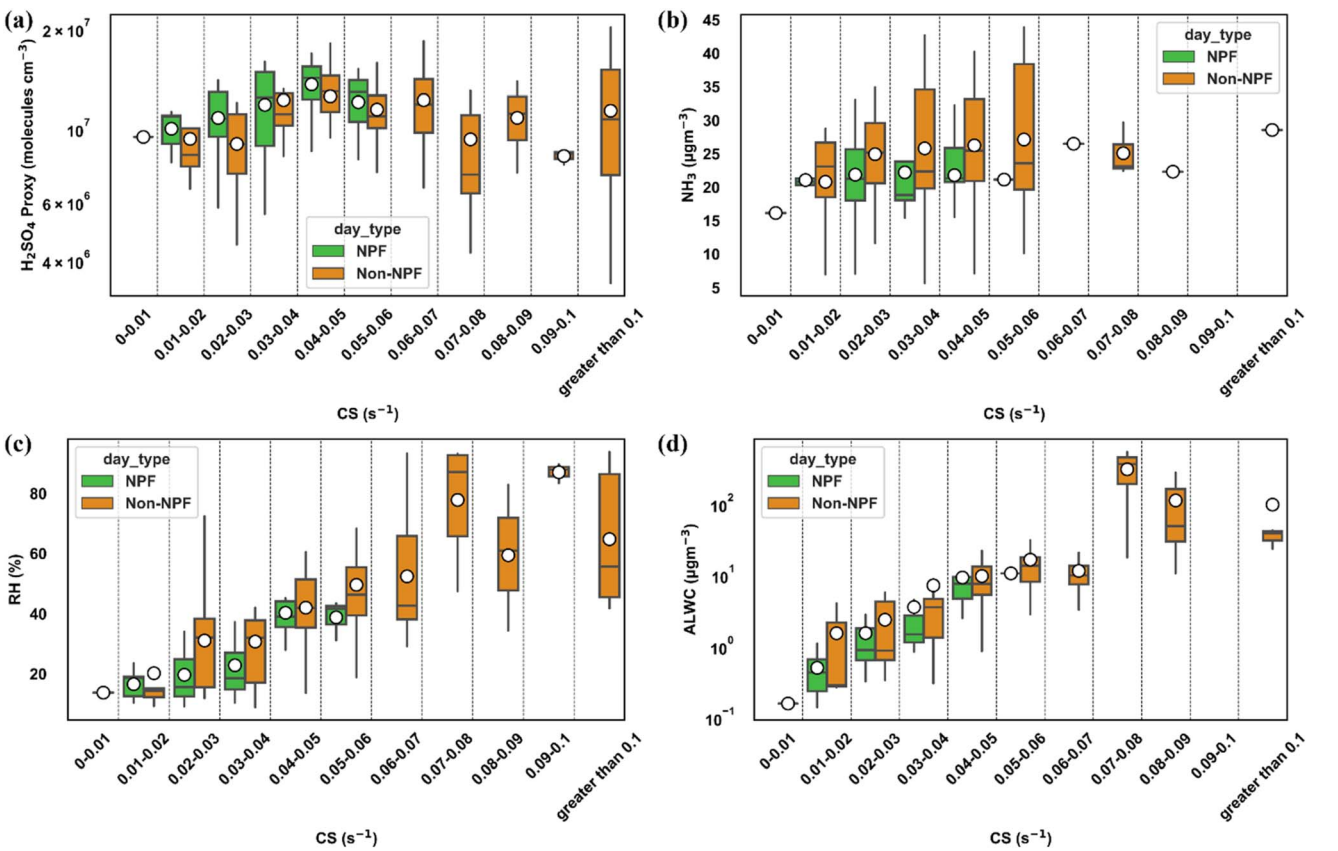

Fig. 5 (a) Average daily variation in the H_2SO_4 proxy concentration (molecules cm^{-3}) *versus* CS (s^{-1}). No new particle formation (NPF) event was observed when the average daytime CS was above 0.06 s^{-1}, primarily observed during colder post-monsoon and winter periods. While H_2SO_4 proxy concentrations were comparatively higher on NPF days, the difference does not appear statistically significant. (b) variation of NH_3 *vs.* CS during NPF and non-NPF days. (c) and (d) Average daytime variation of RH and ALWC (μg m^{-3}) *versus* CS (s^{-1}). In lower CS bins (<0.02 s^{-1}), high ALWC on non-NPF days led to enhancement in CS of particles and consequently hindering NPF. In the moderate CS bins (0.02 to 0.06 s^{-1}), lower RH and lower ALWC favoured NPF. Each data point represents the average of the variable from 10:00 to 16:00 local time (LT).

Fig. 5a compares the average daytime concentration of H_2SO_4 in various CS intervals. The comparison reveals that daytime H_2SO_4 levels were consistently higher on NPF days than on non-NPF days across all CS regimes. Specifically, a notable observation is that most NPF events occur when CS values are on the lower end (<0.03 s^{-1}), accompanied by heightened H_2SO_4 levels in the atmosphere. This highlights the significant role of H_2SO_4 and the lower CS in facilitating NPF in Delhi. However, as CS increases, the variation between NPF and non-NPF days diminishes, particularly in moderate CS regimes (0.03 to 0.06 s^{-1}). This trend is further supported by the comparison of diel variation plots of H_2SO_4 proxy between NPF and non-NPF days in low (<0.03 s^{-1}) and moderate (0.03 to 0.06 s^{-1}) CS regions, as depicted in Fig. S13a and b† (daytime hours variation of H_2SO_4), respectively. These findings suggest that while the sulfuric acid concentration remains an essential factor for NPF, the influence of other vapours, whose precursors may be associated with high particle concentrations, might also contribute to the observed NPF events. In regions with higher CS (>0.06 s^{-1}), we observed either lower or nearly equivalent proxy concentrations of H_2SO_4. This observation could be attributed to reduced or blocked solar radiation or colder seasons when solar radiation is relatively lower than that in summer and spring. However, even in high CS regions, the concentration of gaseous sulfuric acid exceeds 10^6 molecules per cm^3, which is deemed sufficient for NPF in the atmosphere.[90,93,99] Furthermore, we observed higher concentrations of SO_2 during higher CS (Fig. S14a†), the precursor for H_2SO_4, indicating a likely association between elevated SO_2 levels and co-emitted particle concentration. However, the fact that the validity of the proxy used has not been tested under different pollution conditions and seasons still can lead to some uncertainty. This again suggests that sufficient sulfuric acid is consistently present in Delhi across various CS regimes and seasons, indicating that it is not a limiting factor for NPF in the region. However, the high concentration of pre-existing particles acts as a significant sink for H_2SO_4, thereby limiting NPF.

In addition to H_2SO_4, other highly oxygenated molecules (HOMs) or extremely low-volatility organic compounds (ELVOCs) have been found to participate in the continued growth of the newly formed particles.[100–102] Apart from these condensable acidic gases, bases such as ammonia and amines stabilize these critical nuclei in different ambient environments.[37,95,103–105] In both laboratory and field measurements, ammonia and other amines such as dimethylamine (DMA) have been found in critical clusters along with H_2SO_4.[94,95,105,106] During our study, the observed apparent particle formation rate of 10 nm particles (J_{10}) showed an average value of 2.19 ± 0.97 cm^{-3} s^{-1}. The corresponding average daytime $J_{1.5}$ value ranged from 11.6 cm^{-3} s^{-1} to 800 cm^{-3} s^{-1}, with an average value of 136 cm^{-3} s^{-1}. The weak correlation (0.3) between $J_{1.5}$ and the average daytime H_2SO_4 concentration suggests that sulfuric acid alone is not the primary driver of nucleation (Fig. S15†). Furthermore, these formation rates are several magnitudes of order higher than the theoretical nucleation rates predicted from the binary H_2SO_4–H_2O nucleation mechanism. Given the high concentrations of ammonia over Delhi and Indo-Gangetic plains (IGPs),[1,3] nucleation mechanisms involving ammonia are expected to play a significant role. CERN CLOUD experiments involving ammonia and other amines such as DMA at sub ppb levels have found the enhancement by several orders of magnitude in the nucleation rates, with the effect more pronounced in DMA.[37,95,107] However, these ammonia and DMA experiments have not been conducted at temperatures beyond 292 K, exceeding 300 K during our NPF days. Ammonia levels at more than 10 ppb and DMA levels at sub ppb levels have been found to explain the observed high formation rates (~100 cm^{-3} s^{-1}) in polluted environments such as Beijing and Shanghai; however, the observed temperatures are again significantly lower than those in our study.[108,109] However, the fact that the saturation ammonia concentration increases with temperature and whether observed ambient concentrations of ammonia in the (~30 ppb) range will be sufficient to explain the observed nucleation rates will require further investigation. Furthermore, upon investigating the difference in average daytime concentrations of ammonia between NPF and non-NPF days in different CS regions, we observed that ammonia was higher on non-NPF days than on NPF days (Fig. 5b), which suggests that ammonia might not be a limiting factor. Moreover, whether DMA is responsible for the high nucleation rates in Delhi, like other polluted environments, needs further investigation, as necessary measurements to confirm this have still not been made in Delhi.

Other oxygenated organic molecules such as HOMs, formed from the oxidation of volatile organic compounds (VOCs), have been found to participate in the nucleation process.[100,110] Their role may be restricted as a high concentration of NO_x (>30 ppb) is likely to inhibit the formation of HOMs.[111] While we observed a notable increase in O_3 concentrations during NPF event days (Fig. S14b and S16†), it is important to note that high ozone concentrations do not necessarily correlate with high HOM levels, as the formation of HOMs depends on the availability of specific VOC precursors and favourable conditions.[112–114] Nevertheless, the increase in O_3 still suggests the presence of substantial condensable oxygenated organic vapours, such as carboxylic acids,[115] which may significantly impact NPF in this region. Furthermore, whether the gas phase concentration of other condensable vapours such as ammonia, DMA, or dicarboxylic acids is sufficient to play a decisive role in the nucleation process in Delhi needs to be investigated from future field measurements or experiments under comparable atmospheric conditions. In highly polluted areas, one of the explanations for NPF to take place despite the high CS is the participation of another type of vapour, such as organics with higher molecular mass, the primary reason being the concentration of condensable vapours. CS is sensitive to the molecular mass of condensing vapours and decreases with the increasing molecular mass of the vapours.[116,117] Further CS effectiveness decreases with the involvement of ammonia and DMA because alkaline compounds can decrease the saturation vapor pressure of H_2SO_4, thereby enhancing the stability of these critical clusters.

In the moderate CS region (0.03–0.06 s^{-1}), there are days with different characteristics in terms of being an NPF or non-NPF event despite having comparable CS and H_2SO_4 concentrations. The frequency of NPF decreased as CS increased in this region, indicating that CS is still the decisive factor in whether NPF will occur. However, in the moderate CS region, when the CS values are comparable during NPF events and non-NPF days, other factors such as the precursor condensable vapor concentration, photochemical activity, RH, T, or even chemical composition may also play an essential role in driving NPF.

3.4 Role of meteorological parameters

The relationship between meteorological factors and NPF events demonstrates the complex interactions influencing atmospheric chemistry. Fig. 5c shows that daytime RH is higher on non-NPF days across various CS regimes. This shows that RH negatively impacts NPF in our study. Studies have consistently shown that RH is lower on days when NPF occurs compared to days without NPF across both clean and polluted environments.[71,78,118–120] However, the relationship between RH and NPF is not simple to interpret because of the possibility of its impact on NPF in both direct and indirect ways. Water in the atmosphere is crucial for forming initial clusters, whether through binary or ternary nucleation theories.[121] However, under atmospheric conditions, water can also negatively impact the concentration of new particles. This occurs because increased moisture can enhance the aerosol surface area, which in turn can suppress the number of new particles formed.[120] Water condensed on aerosol particles also absorbs gaseous precursor vapours, reducing their availability for particle formation.[118] Additionally, at high RH, the hygroscopic aerosol particles have a higher coagulation efficiency, further inhibiting NPF.[118,122] Furthermore, the relationship is complex because of the interrelationship between RH and T, CS, and solar radiation. Higher RH is usually associated with lower T and can inhibit solar radiation and photochemical reactions essential for NPF.

Fig. S17† shows the variation in T on NPF and non-NPF days across different CS bins. First, the average daytime T shows a negative trend with increasing CS. This shows the positive impact of T on NPF formation, as it is usually associated with low RH and CS. Furthermore, in the same CS bins for CS > 0.02 s^{-1}, the higher average temperature on NPF days compared to non-NPF days also validates the positive impact of T on NPF. In addition to the interrelationship of T with solar radiation and RH, it also directly impacts the NPF process. Temperature can significantly impact the chemical reaction rates of the precursor species along with the emissions of biogenic and anthropogenic VOCs, whose oxidation products play a crucial role in nucleation and the growth of new particles.[123,124] However, in the lower CS region (<0.01 s^{-1}), we observed maximum average temperatures, yet we did not observe any NPF. Despite the sufficient concentration of H_2SO_4 and the low CS, which should have facilitated NPF, no NPF was observed. Additionally, in the CS regime of 0.01 to 0.02 s^{-1}, the average temperature on NPF days was lower compared to non-NPF days. The possible explanation of this might be that the higher temperatures observed on these days might decrease the stability of newly formed nanoclusters.[125] A lower frequency of NPF on days with higher T during the warmer seasons was also observed in a long-term study in Hyytiälä, Finland.[78]

Wind speed can have both beneficial and adverse effects on the occurrence of NPF events. While it can enhance NPF events by promoting the mixing of condensable compounds and reducing the CS, high wind speeds may also hinder NPF events through increased dilution. In low CS regions (CS < 0.03 s^{-1}), wind speeds were generally lower on NPF days compared to non-NPF days, which might have led to the dispersion of condensable vapors needed for new particle formation (Fig. S18a†). In moderate CS regions (0.03 to 0.06 s^{-1}), wind speeds were similar on both NPF and non-NPF days and lower than those in low CS regions (Fig. S18b†). Higher wind speeds in highly polluted areas help remove pre-existing particles, creating favourable conditions for NPF. This trend is evident as wind speeds decreased from low to high CS regimes. However, in the moderate CS regime, no apparent impact of wind speed on NPF can be identified due to the variability in daytime average CS values and other influencing factors.

Furthermore, it is crucial to acknowledge that specific site conditions influence the observed variability in wind speed. Wind speed measurements, particularly in urban areas such as our site, may be affected by local topography or site-specific conditions, thus reflecting local rather than regional conditions for this variable. Therefore, investigating the effect of wind speed on NPF using measurements taken at the measurement site is challenging, as factors beyond wind speed, such as the origin and characteristics of air masses, are also important factors.

3.5 Effect of chemical composition

Chemical composition is another factor that has been found to affect the effectiveness of CS.[17] The effectiveness of heterogeneous nucleation has been shown to strongly depend on the contact angle,[16] which can be influenced by the chemical composition of pre-existing particles, the first step in heterogeneous nucleation. Furthermore, the chemical composition governs the hygroscopic properties of pre-existing particles, which may lead to variation in water uptake and affect the lifetime of condensable vapours such as sulphuric acid, which readily dissolve in water. To identify the possible effect of chemical composition on NPF, we grouped the average $CS_{day\ time}$ into intervals of 0.01 and compared the daytime $PM_{2.5}$ chemical composition of NPF days with those of non-NPF days (Fig. 6a).

We observed the fraction of nitrate and organics increasing as the CS increased, which shows the enhanced contribution of nitrate and organics as pollution levels increased. However, the increase in the organic fraction was more significant. The average organic fraction increased from less than 50% to more than 60% as the average daytime CS increased from 0.01 to 0.1 s^{-1} (Fig. 6a). It is important to note that the absolute concentrations of all species increased with CS, and the increase in

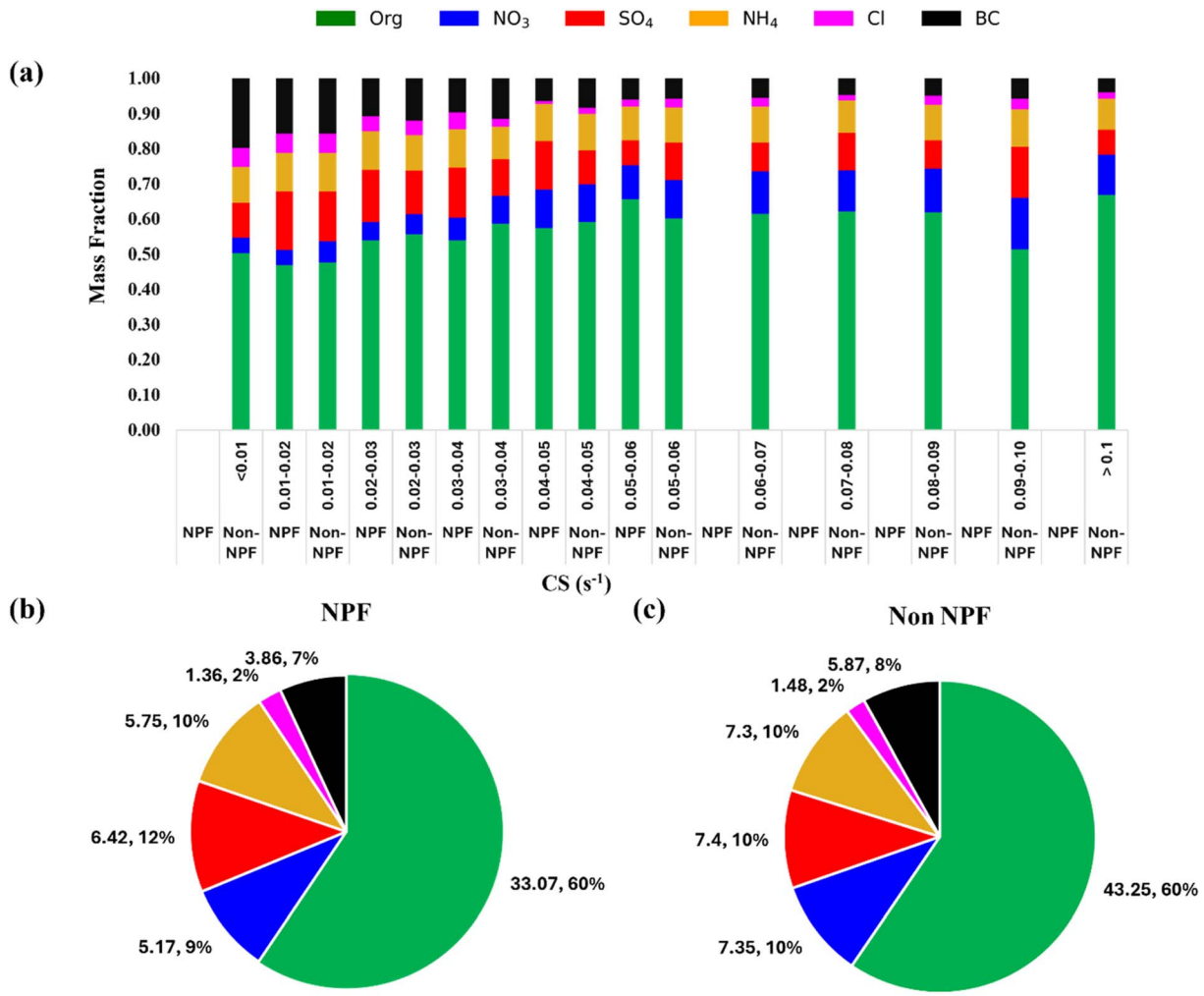

Fig. 6 (a) Comparison of chemical composition of $PM_{2.5}$ during the daytime for NPF and non-NPF days under different CS bins during the daytime; (b) and (c) difference in the chemical composition of $PM_{2.5}$ between NPF and non-NPF days during the days with similar daytime CS and daytime H_2SO_4 vapour concentrations. All the daytime averages have been estimated during the time interval of 10:00 LT to 16:00 LT for each day.

organics does not come at the decrease in concentrations of any other species. Various types of VOCs upon oxidation form condensable organic vapours.[126] These organic compounds have very low volatility and are precursors to secondary organic aerosols. An increase in the organic fraction alongside a higher CS indicates the role of these organic condensable compounds in new particle formation. These molecules cluster with sulphuric acid monomers and increase the molecular mass of clusters which tend to have a larger contact angle, making the heterogeneous nucleation CS less effective.[16,33] This may reduce the effective condensation sink in Delhi and help explain why NPF events occur in Delhi despite the high CS.

Nonetheless, our study lacks measurements of both H_2SO_4, and other compounds associated with NPF in Delhi; consequently, we do not have data on the surface tension and contact angle of these species. Furthermore, the mass composition of $PM_{2.5}$ cannot be directly linked to newly formed particles or initial clusters. However, we can hypothesize about the compounds associated with NPF events.

Furthermore, within the CS interval, we did not observe any significant variations in the overall daytime chemical composition between NPF and non-NPF days. Sulphate was the only component that slightly increased in mass contribution to $PM_{2.5}$ during NPF days for CS below 0.05 s^{-1}. However, the increase was only less than 5% on average. This shows the important role of sulphuric acid in new particle formation-related processes in polluted environments such as Delhi. Organics were the dominant fraction during both NPF and NPF days throughout all CS intervals. This is different from the observations made in Beijing by Du *et al.*[17] and moderately polluted Po Valley (Italy) by Cai *et al.*,[84] where the chemical composition was observed to be different between NPF and non-NPF days, which impacted the CS effectiveness. However, we did not find any difference in the chemical composition between NPF and non-NPF days (Fig. 6b and c), indicating that the chemical composition does not impact the CS effectiveness in Delhi.

The minimal variation in chemical composition between NPF and non-NPF days indicates that the hygroscopicity of particles is similar for both types of days. However, the observed differences in RH between NPF and non-NPF days remain crucial. The hygroscopic growth of particles due to water uptake is an exponential function of RH. Consequently, even with the same chemical composition, higher $PM_{2.5}$ mass concentrations can lead to significant variations in ALWC when there are any notable differences in RH. The observed high RH on non-NPF days compared to NPF days suggests the role of ALWC in enhancing the CS, particularly in the dry CS range of 0.03 to 0.06 s^{-1}. Fig. 5d indicates that aerosol liquid water content increases with condensation sink, with non-NPF days showing higher ALWC at moderate and higher CS values compared to NPF days.

While the hygroscopic growth of pre-existing particles can increase both condensation and coagulation sinks, within the RH range of 40–60%, this growth raises the condensation sink by about 10% (Fig. S19†). This modest increase alone would not explain significantly enhances heterogeneous condensation of vapours based on the increase in size only. Additionally, the increase in the coagulation sinks of nanoclusters due to higher RH has a secondary and rather relatively minor impact on inhibiting NPF.[118] The primary factor remains the reduction in the concentration of sulfuric acid (or any other oxygenated condensable vapour) due to higher RH, either due to a decrease in solar radiation with RH or enhancement in multiphase heterogeneous reactions.

Furthermore, particles can exist in a metastable or stable state depending on their previous RH history. This historical RH influence can affect the CS, even if the current RH does not differ significantly. Although the RH is still below the 40% mark during the daytime, the overnight high RH leads to the metastable state of aerosols (Fig. S17a†), and aerosol particles are still in the aqueous phase, which might enhance the uptake of condensable vapours and CS. We also compared the diel variation of ALWC between NPF and non-NPF days in this moderate CS regime, shown in Fig. S20c.† We observed a higher ALWC mass concentration throughout the day on non-NPF days than on NPF days. During the daytime, the average ALWC mass concentration was about 1.5 times higher on NPF days than that on non-NPF days. Furthermore, the night-time and morning RH preceding the non-NPF events were higher, leading to higher ALWC during those hours. This would promote heterogeneous multiphase reactions, and it can still be in the metastable state during the day it follows.

3.6 New particle formation and condensational growth

The investigation into the chemistry of NPF and growth involves examining the relationship between particle size distribution and the chemical composition of $PM_{2.5}$. As noted in previous studies,[100,127] lower condensable vapours, often low-volatile organic compounds, play an increasingly significant role as particle size increases. This suggests that understanding the contribution of these vapours is crucial for studying the particle growth mechanism. In our study, we utilized a Q-ACSM to measure the mass concentration of $PM_{2.5}$ chemical components over time, specifically focusing on periods of particle growth. By comparing the simultaneous variations in particle size distribution and $PM_{2.5}$ chemical composition, we aim to identify which species are abundant during particle growth and thus likely responsible for the formation and growth of these particles.[21] While Q-ACSM does not capture nucleation mode particles, we can infer the involvement of specific chemical species in particle growth by observing concurrent increases in their mass with particle growth. Additionally, the $PM_{2.5}$ chemical composition differs significantly from that of nucleation mode particles and thus cannot be used to deduce the impacts of organic precursors on NPF, as most $PM_{2.5}$ results from secondary formation through multiphase reactions – a mechanism distinct from nucleation. Our goal is not to claim a comprehensive understanding of the mechanisms underlying the formation or growth of new particles. Instead, we seek to identify the broader sources of vapours that may play a role during different stages of particle growth. During NPF events, where the condensation of gaseous vapours predominantly influences the composition of submicron aerosols, analysing the temporal changes in chemical composition allows us to qualitatively identify the broader vapour sources contributing to new particle growth.[21,128–130] By closely monitoring these temporal changes, we can gain a qualitative understanding of the mechanisms driving NPF and the subsequent growth of particles, thereby enhancing our understanding of the sources and processes contributing to atmospheric particle formation.

Most of the NPF events observed in our study occurred during spring and summer. Also, as CS or PM levels are the determining factors for NPF to occur in Delhi, we divided the spring and summer seasons into polluted and non-polluted days, with the criteria of a daily average of PM_1 as 50 μg m^{-3}. The selection of a daily average of 50 μg m^{-3} as a criterion for PM_1 was made in relation to the $PM_{2.5}$ standard of 60 μg m^{-3}, as set by the Indian National Ambient Air Quality Standards (NAAQS). While the choice is somewhat arbitrary, it reflects a proportional approach based on the difference in particle sizes between PM_1 and $PM_{2.5}$. Since we do not have the mass composition of PM_1, we used the mass composition of $PM_{2.5}$, and the comparison of mass concentration and composition is shown in Fig. 7 and S21† for spring and summer, respectively. It should also be noted that 50 μg m^{-3} set as a criterion for distinguishing polluted and non-polluted is still a high value of PM_1. Still, given the pollution levels in Delhi, this looks like a reasonable assumption since the condensation sink is a dominant primary factor that governs the NPF in Delhi. During the growth period from 10:00 to 16:00 LT, the $PM_{2.5}$ mass concentration decreases, reaching a minimum before increasing again towards the end. A decrease in the mass concentrations of primary components of $PM_{2.5}$, such as BC and primary organics, highlights the impact of the boundary layer and reduced emissions during this time of the day. However, the chemical composition of $PM_{2.5}$ underwent significant changes, as shown in Fig. 7a. As illustrated in Fig. 7a, the contributions of sulphate notably increased, increasing from 12% to 20%. This increase was observed despite the decrease in nitrate and chloride mass fractions, which was attributed to

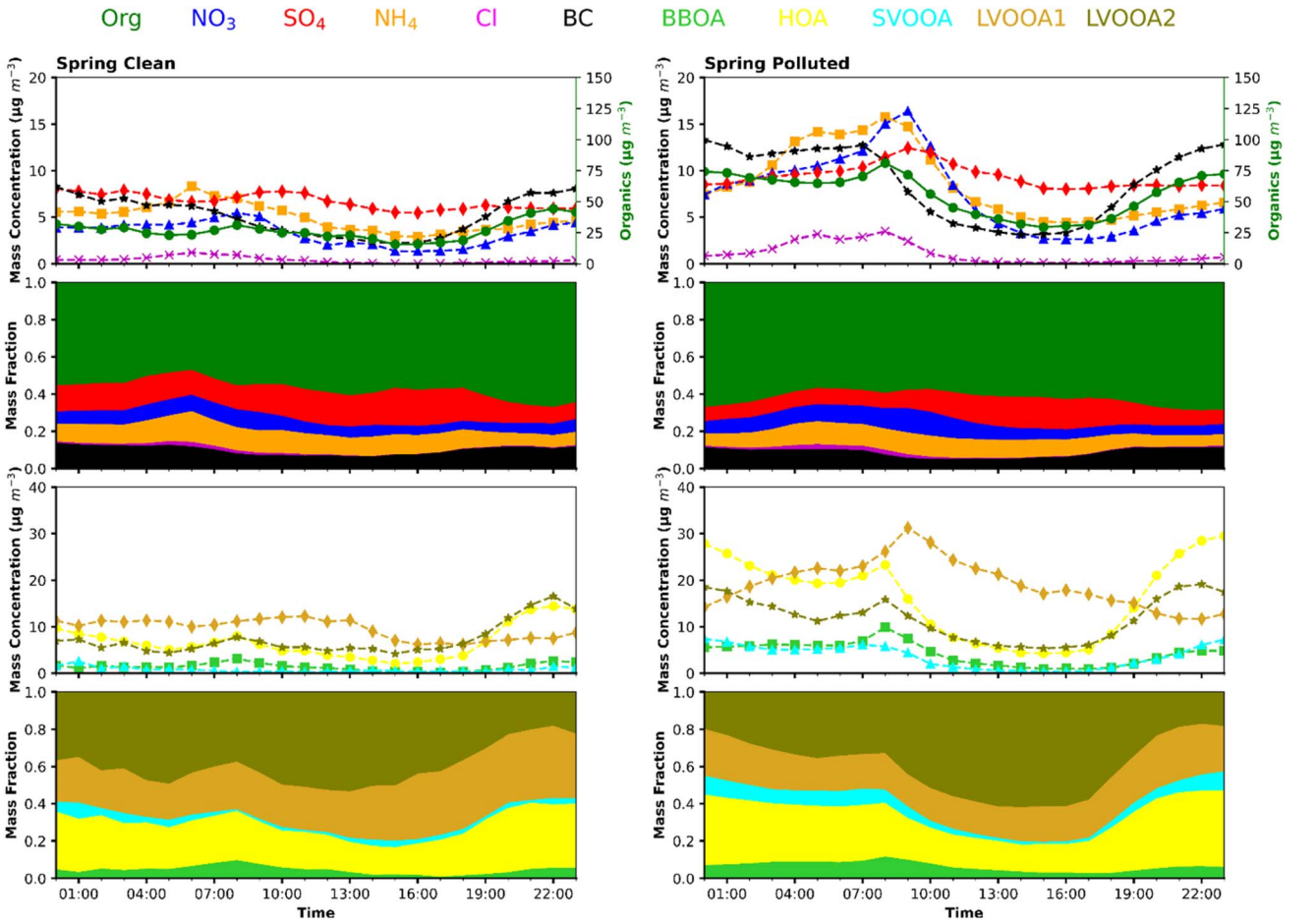

Fig. 7 Diurnal variation of average composition of $PM_{2.5}$ during clean and polluted days of the spring season. Sulphate and oxygenated organic aerosols (LVOOA2) dominated the mass fractions of inorganics and organics, respectively, during the daytime when observed NPF events take place in our study during both clean and polluted periods.

afternoon evaporative losses. This shows that ammonium chloride and nitrate are not involved in the initial condensational growth of newly formed particles. Among the organics, the mass fraction of LVOOA2 (explained in ESI Section S6†) increased from about 30% to more than 50% of the total organics. The fact that every component of $PM_{2.5}$ decreased during the daytime except sulphate and LVOOA2, which show a slight increase or remain constant, shows that daytime oxidation produces abundant condensable vapours of these species, which condense on the existing particles in addition to forming new particles simultaneously. The initiation and further growth of the newly formed particles follow the change in the chemical composition of $PM_{2.5}$, with the contributions of sulphate and more oxidized organics increasing. These findings highlight the significant contribution of low-volatile organic compounds in facilitating nucleated particle growth to climatically relevant sizes, typically exceeding 50 nanometres.

Furthermore, it is essential to note that the sulphate and secondary organic factors were also dominant fractions during the daytime on non-NPF days. Still, the high condensation sink on non-NPF days leads to the condensation of vapours on the existing particles. Even if the particles are formed, they are rapidly scavenged by these larger existing particles.

We further plotted the scatter plots to investigate the relationship between the growth rate (GR) of nucleation mode particles and the CS during NPF events, with an emphasis on the impact of SO_4 and LVOOA2 ratios relative to $PM_{2.5}$ (Fig. S22†). The data points are color-coded to represent these ratios: $SO_4/PM_{2.5}$ in the left plot and $LVOOA2/PM_{2.5}$ in the right plot.

Fig. S22a† on the left shows the scatter plot of the GR (ranging from 3 nm h^{-1} to 10 nm h^{-1}) plotted against CS (from 0.02 s^{-1} to 0.06 s^{-1}), with colours indicating the $SO_4/PM_{2.5}$ ratio (0.100 to 0.250). Similarly, Fig. S22b† presents the same GR and CS values, but with colours representing the $LVOOA2/PM_{2.5}$ ratio (0.20 to 0.45). The provided scatter plots show a wide spread of data points and no clear linear relationship between the growth rate (GR) and condensation sink (CS). This finding was unexpected, given the common assumption that as CS increases, competition for condensation onto existing particles or nucleation of new particles intensifies, leading to a decrease in the GR. The possible explanation may be that as CS increases, the pool of available condensable vapours may ensure that growth rates remain unaffected or even enhanced. This suggests that the condensation sink within the observed range does not predominantly influence the growth rate.

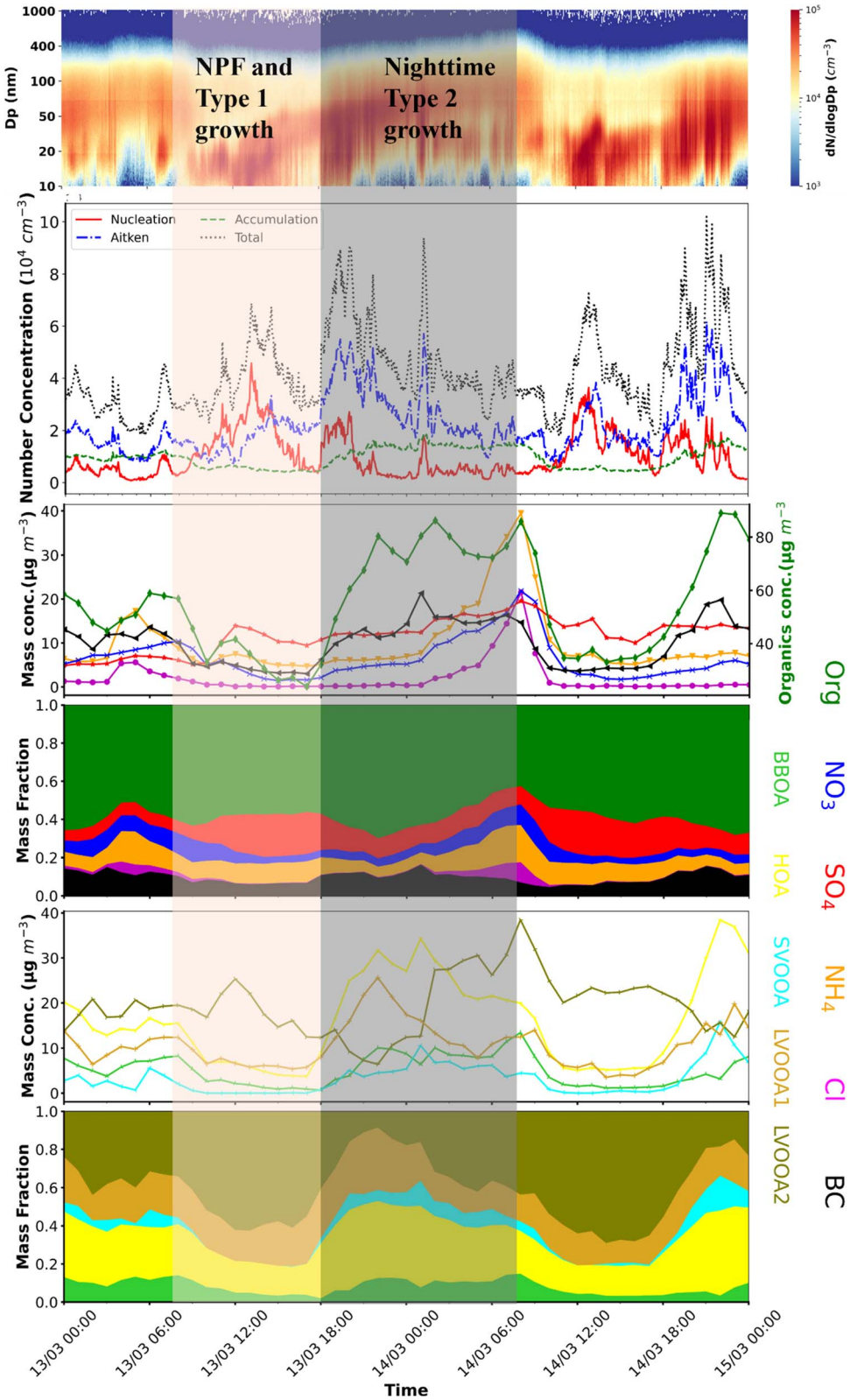

Fig. 8 Temporal variation of particle size distribution, mode PN concentrations, along with chemical composition of $PM_{2.5}$ on two consecutive days, with the first one an NPF. Sulphate and LVOOA2 dominated the mass composition of $PM_{2.5}$ between the periods of start of NPF (10:00 LT and 18:00 LT) and end shaded by the light orange colour in plots. This type I growth is interrupted by primary emissions in the evening hours and undergoes nighttime rapid growth due to coagulation between particles and condensation of vapours resulting from low RH and T, represented by the grey shaded regions in the above plots. The primary nature of these processes is validated by the increase in the mass concentration of BC, HOAs and BBOAs along with their enhancement in mass fractions. Semi volatile inorganics such as nitrate and chloride condense at the later stages of the particle growth.

Furthermore, the color-coded representation reveals that higher $SO_4/PM_{2.5}$ or LVOOA2/$PM_{2.5}$ ratios are distributed across the entire GR and CS value range. This lack of clustering indicates that neither sulphate nor low volatility oxygenated organic aerosols significantly dictates the growth rates of nucleation mode particles in isolation. While SO_4 and LVOOA2 fractions are at their highest during daytime NPF events and dominate $PM_{2.5}$, their ratios do not singularly dictate the growth rates of nucleation mode particles. The findings highlight the need for a more comprehensive approach, incorporating a broader range of variables and interactions to fully understand particle growth mechanisms during NPF events.

While growth often occurs across a wide area through condensation and coagulation processes, local emissions and changes in air chemistry can significantly impact growth patterns, especially in the evening and at night. Increased traffic emissions and lower boundary layers can disrupt typical growth patterns by mixing with existing particles. Fig. 8 shows the temporal variation of chemical composition for two days, one being a typical NPF. At the start of NPF, the mass composition of sulphate and LVOOA2 starts to increase and dominate throughout the first growth stage (~10:00 LT to 18:00 LT). During this time, the mass fraction of primary components such as BC, biomass-burning organic aerosols (BBOAs), and hydrocarbon-like organic aerosols (HOAs), remains lowest. This daytime growth of new particles was disrupted by the simultaneous increase in primary emissions in the evening hours (such as traffic during evening rush hours), residential biomass burning, and a simultaneous decrease in the boundary layer. During the second type of growth, which commences at 18:00 LT, the mass fractions of BC, BBOAs, and HOAs dominate. The nighttime contributions of different primary components to second-type growth further varied season-wise, with BBOAs being the dominant contributors in winter (Fig. S23†) and HOAs dominating during summer and spring seasons. The particle growths observed during this second type of growth differ from the daytime growth as they show higher growth rates, usually higher than the usual 1–10 nm h^{-1} reported worldwide.[71] However, the rapid growth can be attributed to simultaneously experiencing condensation and coagulation in the evening and continuing until the morning of the next day. The decrease in the particle number concentration, while the $PM_{2.5}$ mass concentration increases simultaneously, demonstrates the role of coagulation scavenging. However, the change in chemical composition also shows the role of condensation growth. Furthermore, semi-volatile inorganics such as ammonium nitrate and ammonium chloride condense on these particles in the later stages. The Kelvin effect[131] requires a higher vapor pressure for condensation onto small NPs than onto larger particles.

4. Conclusion

In our study, we investigated the intricate patterns of particle size distribution in Delhi's atmosphere, emphasizing the pivotal role of meteorological phenomena in shaping pollutant dispersion and transformation. We have unveiled significant seasonal variations in particle and PM levels through a comprehensive analysis of one-year-long particle size distribution data alongside measurements of $PM_{2.5}$ chemical composition, trace gases, and meteorological parameters. The persistent dominance of the Aitken mode throughout the year, primarily attributed to traffic emissions, highlights the enduring influence of anthropogenic activities on Delhi's air quality. Additionally, the observed nucleation during warmer seasons, with lower $PM_{2.5}$ mass concentrations, highlights the importance of photochemical radiation and lower CS for gaseous vapours in driving particle formation processes.

Furthermore, our exploration of NPF and the condensational growth process within the context of Delhi's atmospheric pollution has revealed a complex interplay of factors influencing aerosol properties and atmospheric processes. While chemical composition emerged as a critical determinant of NPF and particle growth, with low volatile organic compounds and sulphate playing pivotal roles, CS effectiveness variations were not solely dictated by chemical composition. Factors such as RH and ALWC emerged as crucial influencers, modulating the availability of condensable vapours and altering CS efficacy. Diel variations, particularly during evening and night-time hours, presented additional complexities, with increased local emissions disrupting conventional growth patterns. Simultaneous comparison with mass composition data revealed increased sulphate and oxygenated organic factors during the growth of new particles, indicating the complex interplay between chemical composition and behaviour of particle size distribution. These findings accentuate the importance of sulfuric acid and organic vapours in driving new particle formation.

While our dataset offers valuable insights into nucleation mechanisms, it is important to acknowledge key limitations. The absence of PNSD data for sub-10 nm particles, along with the lack of direct measurements for critical precursor gases such as H_2SO_4, amines, VOCs, and HOMs, limits our ability to fully characterize the factors driving NPF in Delhi. Furthermore, the chemical composition of $PM_{2.5}$, largely influenced by secondary formation processes, differs significantly from nucleation mode particles, complicating the assessment of impacts of organic precursors on NPF.

Acknowledging the complexity of NPF processes, which involve an intricate interplay of meteorological factors, chemical precursors, and physical mechanisms, our study highlights the multifaceted nature of particle nucleation and growth. These processes are difficult to fully characterize without high-resolution measurements of sub-10 nm (or sub-3 nm) particle size distributions and key precursors such as H_2SO_4, amines, VOCs, and HOMs. Although our study does not entirely resolve the mechanistic intricacies of NPF, it establishes a crucial framework for future research. Moreover, it highlights the importance of investigating NPF at the molecular level, specifically adapted to the unique atmospheric conditions of polluted environments in the Global South. This necessitates the use of advanced experimental methodologies to explore the process of new particle formation, from the formation of pre-nucleation clusters to the growth of critical nuclei and nanoparticles.

Data availability

The hourly datasets used in this manuscript will be uploaded to an accessible database upon the manuscript's publication.

Author contributions

Conceptualization: U. A., S. G., and V. S. Data curation: U. A. and M. F. Funding acquisition: V. S. and M. K. Methodology: U. A., S. G., M. F., and V. S. Project administration: M. K. and V. S. Writing – original draft: U. A., S. G., and V. S. Writing – review & editing: all authors.

Conflicts of interest

There are no conflicts to declare.

Acknowledgements

The authors would like to acknowledge the IRD Grand Challenge Project grant from the Indian Institute of Technology Delhi (Grant No. 428 IITD/IRD/MI01810G), under the Ministry of Human Resource Development (MHRD), Government of India, for their financial support in carrying out this work. We also thank our colleagues, Ajit Kumar, Anjanay Pandey, Sombir Pannu, Asad Abbas, Sayan Banerjee, and Amir Ali, for their valuable discussions and contributions.

References

1 P. Acharja, K. Ali, S. D. Ghude, V. Sinha, B. Sinha, R. Kulkarni, *et al.*, Enhanced secondary aerosol formation driven by excess ammonia during fog episodes in Delhi, India, *Chemosphere*, 2022, **289**, 133155.

2 S. S. Gunthe, P. Liu, U. Panda, S. S. Raj, A. Sharma, E. Darbyshire, *et al.*, Enhanced aerosol particle growth sustained by high continental chlorine emission in India, *Nat. Geosci.*, 2021, **14**(2), 77–84.

3 U. Ali, M. Faisal, D. Ganguly, M. Kumar and V. Singh, Analysis of aerosol liquid water content and its role in visibility reduction in Delhi, *Sci. Total Environ.*, 2023, **867**, 161484.

4 S. Gani, S. Bhandari, S. Seraj, D. S. Wang, K. Patel, P. Soni, *et al.*, Submicron aerosol composition in the world's most polluted megacity: the Delhi Aerosol Supersite study, *Atmos. Chem. Phys.*, 2019, **19**(10), 6843–6859.

5 M. Faisal, N. Hazarika, D. Ganguly, M. Kumar and V. Singh, $PM_{2.5}$ bound species variation and source characterization in the post-lockdown period of the Covid-19 pandemic in Delhi, *Urban Climate*, 2022, **46**, 101290.

6 S. Gani, S. Bhandari, K. Patel, S. Seraj, P. Soni, Z. Arub, *et al.*, Particle number concentrations and size distribution in a polluted megacity: the Delhi Aerosol Supersite study, *Atmos. Chem. Phys.*, 2020, **20**(14), 8533–8549.

7 Ü. A. Şahin, R. M. Harrison, M. S. Alam, D. C. S. Beddows, D. Bousiotis, Z. Shi, *et al.*, Measurement report: interpretation of wide-range particulate matter size distributions in Delhi, *Atmos. Chem. Phys.*, 2022, **22**(8), 5415–5433.

8 M. Kulmala, H. Vehkamäki, T. Petäjä, M. Dal Maso, A. Lauri, V. M. Kerminen, *et al.*, Formation and growth rates of ultrafine atmospheric particles: a review of observations, *J. Aerosol Sci.*, 2004, **35**(2), 143–176.

9 M. Kulmama, T. Petäjä, V. M. Kerminen, J. Kujansuu, T. Ruuskanen, A. Ding, *et al.*, On secondary new particle formation in China, *Front. Environ. Sci. Eng.*, 2016, **10**(5), 1–10.

10 M. Kulmala, V. M. Kerminen, T. Petäjä, A. J. Ding and L. Wang, Atmospheric gas-to-particle conversion: why NPF events are observed in megacities?, *Faraday Discuss.*, 2017, **200**, 271–288, DOI: **10.1039/C6FD00257A**.

11 P. Mönkkönen, I. K. Koponen, K. E. J. Lehtinen, K. Hämeri, R. Uma and M. Kulmala, Measurements in a highly polluted Asian mega city: observations of aerosol number size distribution, modal parameters and nucleation events, *Atmos. Chem. Phys.*, 2005, **5**, 57–66, available from: **https://www.atmos-chem-phys.org/acp/5/57/SRef-ID:1680-7324/acp/2005-5-57EuropeanGeosciencesUnion**.

12 B. Sarangi, S. G. Aggarwal, B. Kunwar, S. Kumar, R. Kaur, D. Sinha, *et al.*, Nighttime particle growth observed during spring in New Delhi: evidences for the aqueous phase oxidation of SO_2, *Atmos. Environ.*, 2018, **188**, 82–96.

13 S. K. Yadav, S. K. Kompalli, B. R. Gurjar and R. K. Mishra, Aerosol number concentrations and new particle formation events over a polluted megacity during the COVID-19 lockdown, *Atmos. Environ.*, 2021, **259**, 118526.

14 B. Sarangi, S. G. Aggarwal, D. Sinha and P. K. Gupta, Aerosol effective density measurement using scanning mobility particle sizer and quartz crystal microbalance with the estimation of involved uncertainty, *Atmos. Meas. Tech.*, 2016, **9**(3), 859–875.

15 M. Sebastian, S. K. Kompalli, V. A. Kumar, S. Jose, S. S. Babu, G. Pandithurai, *et al.*, Observations of particle number size distributions and new particle formation in six Indian locations, *Atmos. Chem. Phys.*, 2022, **22**(7), 4491–4508.

16 S. Tuovinen, J. Kontkanen, J. Jiang and M. Kulmala, Investigating the effectiveness of condensation sink based on heterogeneous nucleation theory, *J. Aerosol Sci.*, 2020, **149**, 105613.

17 W. Du, J. Cai, F. Zheng, C. Yan, Y. Zhou, Y. Guo, *et al.*, Influence of Aerosol Chemical Composition on Condensation Sink Efficiency and New Particle Formation in Beijing, *Environ. Sci. Technol. Lett.*, 2022, **9**(5), 375–382.

18 S. Mishra, S. N. Tripathi, V. P. Kanawade, S. L. Haslett, L. Dada, G. Ciarelli, *et al.*, Rapid night-time nanoparticle growth in Delhi driven by biomass-burning emissions, *Nat. Geosci.*, 2023, **16**(3), 224–230.

19 C. Manchanda, M. Kumar and V. Singh, Meteorology governs the variation of Delhi's high particulate-bound chloride levels, *Chemosphere*, 2022, **291**, 132879.

20 M. Faisal, U. Ali, A. Kumar, N. Hazarika, V. Singh and M. Kumar, Festive fireworks in Delhi: a major source of elemental aerosols established through dispersion

normalized PMF in a multiyear study, *Atmos. Environ.*, 2024, **323**, 120394.
21 Y. Zhang, W. Du, Y. Wang, Q. Wang, H. Wang, H. Zheng, *et al.*, Aerosol chemistry and particle growth events at an urban downwind site in North China Plain, *Atmos. Chem. Phys.*, 2018, **18**(19), 14637–14651.
22 M. Masiol, T. V. Vu, D. C. S. Beddows and R. M. Harrison, Source apportionment of wide range particle size spectra and black carbon collected at the airport of Venice (Italy), *Atmos. Environ.*, 2016, **139**, 56–74.
23 T. Wu and B. E. Boor, Urban aerosol size distributions: a global perspective, *Atmos. Chem. Phys.*, 2021, **21**, 8883–8914.
24 M. Dal Maso, M. Kulmala, I. Riipinen, R. Wagner, T. Hussein, P. P. Aalto, *et al.*, *Formation and growth of fresh atmospheric aerosols: eight years of aerosol size distribution data from SMEAR II*, Hyytiälä, Finland, 2005.
25 M. Kulmala, T. Petäjä, T. Nieminen, M. Sipilä, H. E. Manninen, K. Lehtipalo, *et al.*, Measurement of the nucleation of atmospheric aerosol particles, *Nat. Protoc.*, 2012, **7**(9), 1651–1667.
26 J. Pey, X. Querol, A. Alastuey, S. Rodríguez, J. P. Putaud and R. Van Dingenen, Source apportionment of urban fine and ultra-fine particle number concentration in a Western Mediterranean city, *Atmos. Environ.*, 2009, **43**(29), 4407–4415, available from: **https://www.sciencedirect.com/science/article/pii/S1352231009004531**.
27 N. Kulmala, *On the mode-segregated aerosol particle number concentration load: contributions of primary and secondary particles in Hyytiälä and Nanjing*, 2016, available from: **http://hdl.handle.net/10138/165340**.
28 M. Kulmala, M. Dal Maso, J. M. Mäkelä, M. Mäkela, M. Mäkelä and L. Pirjola, On the formation, growth and composition of nucleation mode particles, *Tellus B*, 2001, **53**, 479–490.
29 E. N. Fuller, K. Ensley and J. C. Giddings, Diffusion of halogenated hydrocarbons in helium. The effect of structure on collision cross sections, *J. Phys. Chem.*, 1969, **73**, 3679–3685.
30 E. N. Fuller, P. D. Schettler and J. C. Giddings, New method for prediction of binary gas-phase diffusion coefficients, *Ind. Eng. Chem.*, 1966, **58**(5), 18–27, DOI: **10.1021/ie50677a007**.
31 R. C. Reid, J. M. Prausnitz and B. E. Poling, *The properties of gases and liquids*, McGraw Hill Book Co., New York, USA, 1987, available from: **https://www.osti.gov/biblio/6504847**.
32 N. A. Fuchs and A. G. Sutugin. High-dispersed aerosols, in *Topics in Current Aerosol Research*, ed. G. M. Hidy and J. R. Brock, Pergamon, 1971, p. 1, International Reviews in Aerosol Physics and Chemistry, available from: **https://www.sciencedirect.com/science/article/pii/B9780080166742500066**.
33 S. Tuovinen, J. Kontkanen, R. Cai and M. Kulmala, Condensation sink of atmospheric vapors: the effect of vapor properties and the resulting uncertainties, *Environ. Sci.: Atmos.*, 2021, **1**(7), 543–557.
34 T. Hussein and M. Dal Maso, *Evaluation of an automatic algorithm for fitting the particle number size distribution*, 2005, available from: **https://www.researchgate.net/publication/227944272**.
35 M. Kulmala, I. Riipinen, M. Sipilä, H. E. Manninen, T. Petäjä, H. Junninen, *et al.*, Toward Direct Measurement of Atmospheric Nucleation, *Science*, 2007, **318**(5847), 89–92, DOI: **10.1126/science.1144124**.
36 R. Zhang, Getting to the Critical Nucleus of Aerosol Formation, *Science*, 2010, **328**(5984), 1366–1367, DOI: **10.1126/science.1189732**.
37 J. Kirkby, J. Curtius, J. Almeida, E. Dunne, J. Duplissy, S. Ehrhart, *et al.*, Role of sulphuric acid, ammonia and galactic cosmic rays in atmospheric aerosol nucleation, *Nature*, 2011, **476**(7361), 429–435.
38 V. M. Kerminen and M. Kulmala, Analytical formulae connecting the "real" and the "apparent" nucleation rate and the nuclei number concentration for atmospheric nucleation events, *J. Aerosol Sci.*, 2002, **33**(4), 609–622, available from: **https://www.sciencedirect.com/science/article/pii/S002185020100194X**.
39 M. Kulmala, K. E. J. Lehtinen and A. Laaksonen, Cluster activation theory as an explanation of the linear dependence between formation rate of 3 nm particles and sulphuric acid concentration, *Atmos. Chem. Phys.*, 2006, **6**, 787–793, available from: **https://www.atmos-chem-phys.net/6/787/2006/**.
40 H. Korhonen, S. L. Sihto, V. M. Kerminen and K. E. J. Lehtinen, Evaluation of the accuracy of analysis tools for atmospheric new particle formation, *Atmos. Chem. Phys.*, 2011, **11**(7), 3051–3066, available from: **https://acp.copernicus.org/articles/11/3051/2011/**.
41 M. Kulmala, J. Kontkanen, H. Junninen, K. Lehtipalo, H. E. Manninen, T. Nieminen, *et al.*, Direct Observations of Atmospheric Aerosol Nucleation, *Science*, 2013, **339**(6122), 943–946, DOI: **10.1126/science.1227385**.
42 L. Dada, I. Ylivinkka, R. Baalbaki, C. Li, Y. Guo, C. Yan, *et al.*, Sources and sinks driving sulfuric acid concentrations in contrasting environments: implications on proxy calculations, *Atmos. Chem. Phys.*, 2020, **20**(20), 11747–11766.
43 T. Petäjä, I. I. I. R. L. Mauldin, E. Kosciuch, J. McGrath, T. Nieminen, P. Paasonen, *et al.*, Sulfuric acid and OH concentrations in a boreal forest site, *Atmos. Chem. Phys.*, 2009, **9**(19), 7435–7448, available from: **https://acp.copernicus.org/articles/9/7435/2009/**.
44 S. Mikkonen, S. Romakkaniemi, J. N. Smith, H. Korhonen, T. Petäjä, C. Plass-Duelmer, *et al.*, A statistical proxy for sulphuric acid concentration, *Atmos. Chem. Phys.*, 2011, **11**(21), 11319–11334, available from: **https://acp.copernicus.org/articles/11/11319/2011/**.
45 L. Dada, I. Ylivinkka, R. Baalbaki, C. Li, Y. Guo, C. Yan, *et al.*, Sources and sinks driving sulfuric acid concentrations in contrasting environments: implications on proxy calculations, *Atmos. Chem. Phys.*, 2020, **20**(20), 11747–11766, available from: **https://acp.copernicus.org/articles/20/11747/2020/**.

46 Y. Lu, C. Yan, Y. Fu, Y. Chen, Y. Liu, G. Yang, *et al.*, A proxy for atmospheric daytime gaseous sulfuric acid concentration in urban Beijing, *Atmos. Chem. Phys.*, 2019, **19**(3), 1971–1983, available from: https://acp.copernicus.org/articles/19/1971/2019/.

47 H. Berresheim, T. Elste, H. G. Tremmel, A. G. Allen, H. C. Hansson, K. Rosman, *et al.*, Gas-aerosol relationships of H_2SO_4, MSA, and OH: observations in the coastal marine boundary layer at Mace Head, Ireland, *J. Geophys. Res.: Atmos.*, 2002, **107**(19), PAR 5-1–PAR 5-12.

48 X. Zhang, Y. Zhang, J. Sun, X. Zheng, G. Li and Z. Deng, Characterization of particle number size distribution and new particle formation in an urban environment in Lanzhou, China, *J. Aerosol Sci.*, 2017, **103**, 53–66.

49 Z. Wu, M. Hu, P. Lin, S. Liu, B. Wehner and A. Wiedensohler, Particle number size distribution in the urban atmosphere of Beijing, China, *Atmos. Environ.*, 2008, **42**(34), 7967–7980.

50 T. Hussein, A. Puustinen, P. P. Aalto, J. M. Mäkelä, K. Hämeri and M. Kulmala, Urban aerosol number size distributions, *Atmos. Chem. Phys.*, 2004, **4**, 391–411, available from: https://www.atmos-chem-phys.org/acp/4/391/.

51 Y. Zhang, W. Du, Y. Wang, Q. Wang, H. Wang, H. Zheng, *et al.*, Aerosol chemistry and particle growth events at an urban downwind site in North China Plain, *Atmos. Chem. Phys.*, 2018, **18**(19), 14637–14651.

52 S. Yang, Z. Liu, P. S. Clusius, Y. Liu, J. Zou, Y. Yang, *et al.*, Chemistry of new particle formation and growth events during wintertime in suburban area of Beijing: insights from highly polluted atmosphere, *Atmos. Res.*, 2021, **255**, 105553.

53 J. Chen, C. Li, Z. Ristovski, A. Milic, Y. Gu, M. S. Islam, *et al.*, A review of biomass burning: Emissions and impacts on air quality, health and climate in China, *Sci. Total Environ.*, 2017, **579**, 1000–1034.

54 P. Kumar, L. Pirjola, M. Ketzel and R. M. Harrison, Nanoparticle emissions from 11 non-vehicle exhaust sources - a review, *Atmos. Environ.*, 2013, **67**, 252–277.

55 P. Paasonen, K. Kupiainen, Z. Klimont, A. Visschedijk, H. A. C. D. Van Der Gon and M. Amann, Continental anthropogenic primary particle number emissions, *Atmos. Chem. Phys.*, 2016, **16**(11), 6823–6840.

56 V. Riffault, J. Arndt, H. Marris, S. Mbengue, A. Setyan, L. Y. Alleman, *et al.*, Fine and ultrafine particles in the vicinity of industrial activities: a review, *Crit. Rev. Environ. Sci. Technol.*, 2015, **45**(21), 2305–2356.

57 Y. Zhu, W. C. Hinds, S. Kim and C. Sioutas, Concentration and size distribution of ultrafine particles near a major highway, *J. Air Waste Manage. Assoc.*, 2002, **52**(9), 1032–1042.

58 N. G. Kim, S. B. Jeong, H. C. Jin, J. Lee, K. H. Kim, S. Kim, *et al.*, Spatial and PMF analysis of particle size distributions simultaneously measured at four locations at the roadside of highways, *Sci. Total Environ.*, 2023, **893**, 164892.

59 S. Gani, S. Bhandari, K. Patel, S. Seraj, P. Soni, Z. Arub, *et al.*, Particle number concentrations and size distribution in a polluted megacity: the Delhi Aerosol Supersite study, *Atmos. Chem. Phys.*, 2020, **20**(14), 8533–8549, available from: https://acp.copernicus.org/articles/20/8533/2020/.

60 M. Kulmala, H. Vehkamäki, T. Petäjä, M. Dal Maso, A. Lauri, V. M. Kerminen, *et al.*, Formation and growth rates of ultrafine atmospheric particles: a review of observations, *J. Aerosol Sci.*, 2004, **35**(2), 143–176.

61 S. Jose, A. K. Mishra, N. K. Lodhi, S. K. Sharma and S. Singh, Characteristics of Aerosol Size Distributions and New Particle Formation Events at Delhi: An Urban Location in the Indo-Gangetic Plains, *Front. Earth Sci.*, 2021, **9**, 750111.

62 T. Nieminen, V. M. Kerminen, T. Petäjä, P. P. Aalto, M. Arshinov, E. Asmi, *et al.*, Global analysis of continental boundary layer new particle formation based on long-term measurements, *Atmos. Chem. Phys.*, 2018, **18**(19), 14737–14756.

63 Z. Wu, M. Hu, S. Liu, B. Wehner, S. Bauer, A. Ma ßLing, *et al.*, New particle formation in Beijing, China: statistical analysis of a 1-year data set, *J. Geophys. Res.: Atmos.*, 2007, **112**(9), DOI: 10.1029/2006JD007406.

64 V. P. Kanawade, S. N. Tripathi, D. Siingh, A. S. Gautam, A. K. Srivastava, A. K. Kamra, *et al.*, Observations of new particle formation at two distinct Indian subcontinental urban locations, *Atmos. Environ.*, 2014, **96**, 370–379.

65 S. S. Babu, S. K. Kompalli and K. K. Moorthy, Aerosol number size distributions over a coastal semi urban location: seasonal changes and ultrafine particle bursts, *Sci. Total Environ.*, 2016, **563–564**, 351–365.

66 W. Du, L. Dada, J. Zhao, X. Chen, K. R. Daellenbach, C. Xie, *et al.*, A 3D study on the amplification of regional haze and particle growth by local emissions, *npj Clim. Atmos. Sci.*, 2021, **4**(1), 4.

67 G. J. Roelofs, P. Stier, J. Feichter, E. Vignati and J. Wilson, Aerosol activation and cloud processing in the global aerosol-climate model ECHAM5-HAM, *Atmos. Chem. Phys.*, 2006, **6**, 2389–2399, available from: https://www.atmos-chem-phys.net/6/2389/2006/.

68 J. Ren, L. Chen, T. Fan, J. Liu, S. Jiang and F. Zhang, The NPF Effect on CCN Number Concentrations: A Review and Re-Evaluation of Observations from 35 Sites Worldwide, *Geophys. Res. Lett.*, 2021, **48**(19), e2021GL095190.

69 M. Kulmala, R. Cai, D. Stolzenburg, Y. Zhou, L. Dada, Y. Guo, *et al.*, The contribution of new particle formation and subsequent growth to haze formation, *Environ. Sci.: Atmos.*, 2022, **2**(3), 352–361.

70 R. Zhang, A. Khalizov, L. Wang, M. Hu and W. Xu, Nucleation and growth of nanoparticles in the atmosphere, *Chem. Rev.*, 2012, **112**, 1957–2011.

71 V. M. Kerminen, X. Chen, V. Vakkari, T. Petäjä, M. Kulmala and F. Bianchi, Atmospheric new particle formation and growth: review of field observations, *Environ. Res. Lett.*, 2018, **13**, 103003.

72 W. Birmili, A. Wiedensohler, C. Plass-Dülmer and H. Berresheim, Evolution of newly formed aerosol particles in the continental boundary layer: a case study including OH and H_2SO_4 measurements, *Geophys. Res. Lett.*, 2000, **27**(15), 2205–2208.

73 C. Kuang, I. Riipinen, S. L. Sihto, M. Kulmala, A. V. McCormick and P. H. McMurry, An improved criterion for new particle formation in diverse atmospheric environments, *Atmos. Chem. Phys.*, 2010, **10**(17), 8469–8480.
74 M. Kulmala, T. Petäjä, M. Ehn, J. Thornton, M. Sipilä, D. R. Worsnop, *et al.*, Chemistry of atmospheric nucleation: on the recent advances on precursor characterization and atmospheric cluster composition in connection with atmospheric new particle formation, *Annu. Rev. Phys. Chem.*, 2014, **65**, 21–37.
75 M. Kulmala and V. M. Kerminen, On the formation and growth of atmospheric nanoparticles, *Atmos. Res.*, 2008, **90**(2–4), 132–150.
76 M. Kulmala, V. M. Kerminen, T. Petäjä, A. J. Ding and L. Wang, Atmospheric gas-to-particle conversion: why NPF events are observed in megacities?, *Faraday Discuss.*, 2017, **200**, 271–288.
77 E. Asmi, N. Kivekäs, V. M. Kerminen, M. Komppula, A. P. Hyvärinen, J. Hatakka, *et al.*, Secondary new particle formation in Northern Finland Pallas site between the years 2000 and 2010, *Atmos. Chem. Phys.*, 2011, **11**(24), 12959–12972.
78 L. Dada, P. Paasonen, T. Nieminen, S. Buenrostro Mazon, J. Kontkanen, O. Peräkylä, *et al.*, Long-term analysis of clear-sky new particle formation events and nonevents in Hyytiälä, *Atmos. Chem. Phys.*, 2017, **17**(10), 6227–6241.
79 L. Dai, H. Wang, L. Zhou, J. An, L. Tang, C. Lu, *et al.*, Regional and local new particle formation events observed in the Yangtze River Delta region, China, *J. Geophys. Res.*, 2017, **122**(4), 2389–2402.
80 V. P. Kanawade, S. N. Tripathi, D. Siingh, A. S. Gautam, A. K. Srivastava, A. K. Kamra, *et al.*, Observations of new particle formation at two distinct Indian subcontinental urban locations, *Atmos. Environ.*, 2014, **96**, 370–379.
81 I. Salma, T. Borsòs, T. Weidinger, P. Aalto, T. Hussein, M. Dal Maso, *et al.*, Production, growth and properties of ultrafine atmospheric aerosol particles in an urban environment, *Atmos. Chem. Phys.*, 2011, **11**(3), 1339–1353.
82 L. Dada, P. Paasonen, T. Nieminen, S. Buenrostro Mazon, J. Kontkanen, O. Peräkylä, *et al.*, Long-term analysis of clear-sky new particle formation events and nonevents in Hyytiälä, *Atmos. Chem. Phys.*, 2017, **17**(10), 6227–6241.
83 I. Salma, Z. Németh, V. M. Kerminen, P. Aalto, T. Nieminen, T. Weidinger, *et al.*, Regional effect on urban atmospheric nucleation, *Atmos. Chem. Phys.*, 2016, **16**(14), 8715–8728, available from: **https://acp.copernicus.org/articles/16/8715/2016/**.
84 J. Cai, J. Sulo, Y. Gu, S. Holm, R. Cai, S. Thomas, *et al.*, Elucidating the mechanisms of atmospheric new particle formation in the highly polluted Po Valley, Italy, *Atmos. Chem. Phys.*, 2024, **24**(4), 2423–2441, available from: **https://acp.copernicus.org/articles/24/2423/2024/**.
85 J. Brean, D. C. S. Beddows, R. M. Harrison, C. Song, P. Tunved, J. Ström, *et al.*, Collective geographical ecoregions and precursor sources driving Arctic new particle formation, *Atmos. Chem. Phys.*, 2023, **23**(3), 2183–2198, available from: **https://acp.copernicus.org/articles/23/2183/2023/**.
86 S. Lai, X. Qi, X. Huang, S. Lou, X. Chi, L. Chen, *et al.*, New particle formation induced by anthropogenic–biogenic interactions on the southeastern Tibetan Plateau, *Atmos. Chem. Phys.*, 2024, **24**(4), 2535–2553, available from: **https://acp.copernicus.org/articles/24/2535/2024/**.
87 M. O. Andreae, T. W. Andreae, F. Ditas and C. Pöhlker, Frequent new particle formation at remote sites in the subboreal forest of North America, *Atmos. Chem. Phys.*, 2022, **22**(4), 2487–2505, available from: **https://acp.copernicus.org/articles/22/2487/2022/**.
88 Y. Wang and Y. Chen, Significant Climate Impact of Highly Hygroscopic Atmospheric Aerosols in Delhi, India, *Geophys. Res. Lett.*, 2019, **46**(10), 5535–5545.
89 S. S. Gunthe, P. Liu, U. Panda, S. S. Raj, A. Sharma, E. Darbyshire, *et al.*, Enhanced aerosol particle growth sustained by high continental chlorine emission in India, *Nat. Geosci.*, 2021, **14**(2), 77–84.
90 T. Nieminen, H. E. Manninen, S. L. Sihto, T. Yli-Juuti, R. L. Mauldin, T. Petäjä, *et al.*, Connection of sulfuric acid to atmospheric nucleation in boreal forest, *Environ. Sci. Technol.*, 2009, **43**(13), 4715–4721.
91 C. Kuang, P. H. McMurry, A. V. McCormick and F. L. Eisele, Dependence of nucleation rates on sulfuric acid vapor concentration in diverse atmospheric locations, *J. Geophys. Res.: Atmos.*, 2008, **113**(D10), DOI: **10.1029/2007JD009253**.
92 P. H. McMurry, M. Fink, H. Sakurai, M. R. Stolzenburg, I. L. Mauldin, J. Smith, *et al.*, A criterion for new particle formation in the sulfur-rich Atlanta atmosphere, *J. Geophys. Res.: Atmos.*, 2005, **110**(22), 1–10.
93 M. E. Erupe, D. R. Benson, J. Li, L. H. Young, B. Verheggen, M. Al-Refai, *et al.*, Correlation of aerosol nucleation rate with sulfuric acid and ammonia in Kent, Ohio: an atmospheric observation, *J. Geophys. Res.: Atmos.*, 2010, **115**(D23), DOI: **10.1029/2010JD013942**.
94 S. H. Lee, H. Gordon, H. Yu, K. Lehtipalo, R. Haley, Y. Li, *et al.*, New Particle Formation in the Atmosphere: From Molecular Clusters to Global Climate, *J. Geophys. Res.: Atmos.*, 2019, **124**, 7098–7146.
95 J. Almeida, S. Schobesberger, A. Kürten, I. K. Ortega, O. Kupiainen-Määttä, A. P. Praplan, *et al.*, Molecular understanding of sulphuric acid-amine particle nucleation in the atmosphere, *Nature*, 2013, **502**(7471), 359–363.
96 J. Zhao, J. N. Smith, F. L. Eisele, M. Chen, C. Kuang and P. H. McMurry, Observation of neutral sulfuric acid-amine containing clusters in laboratory and ambient measurements, *Atmos. Chem. Phys.*, 2011, **11**(21), 10823–10836.
97 R. J. Weber, J. J. Marti, P. H. McMurry, F. L. Eisele, D. J. Tanner and A. Jefferson, Measurements of new particle formation and ultrafine particle growth rates at a clean continental site, *J. Geophys. Res.: Atmos.*, 1997, **102**(4), 4375–4385.

98 C. Kuang, P. H. McMurry, A. V. McCormick and F. L. Eisele, Dependence of nucleation rates on sulfuric acid vapor concentration in diverse atmospheric locations, *J. Geophys. Res.: Atmos.*, 2008, **113**(D10), DOI: **10.1029/2007JD009253**.

99 P. H. McMurry, M. Fink, H. Sakurai, M. R. Stolzenburg, I. L. Mauldin, J. Smith, *et al.*, A criterion for new particle formation in the sulfur-rich Atlanta atmosphere, *J. Geophys. Res.: Atmos.*, 2005, **110**(22), 1–10.

100 M. Ehn, J. A. Thornton, E. Kleist, M. Sipilä, H. Junninen, I. Pullinen, *et al.*, A large source of low-volatility secondary organic aerosol, *Nature*, 2014, **506**(7489), 476–479.

101 T. Nieminen, V. M. Kerminen, T. Petäjä, P. P. Aalto, M. Arshinov, E. Asmi, *et al.*, Global analysis of continental boundary layer new particle formation based on long-term measurements, *Atmos. Chem. Phys.*, 2018, **18**(19), 14737–14756.

102 P. Paasonen, T. Nieminen, E. Asmi, H. E. Manninen, T. Petäjä, C. Plass-Dülmer, *et al.*, On the roles of sulphuric acid and low-volatility organic vapours in the initial steps of atmospheric new particle formation, *Atmos. Chem. Phys.*, 2010, **10**(22), 11223–11242.

103 J. Zheng, Y. Ma, M. Chen, Q. Zhang, L. Wang, A. F. Khalizov, *et al.*, Measurement of atmospheric amines and ammonia using the high resolution time-of-flight chemical ionization mass spectrometry, *Atmos. Environ.*, 2015, **102**, 249–259.

104 R. Zhang, P. J. Wooldridge, J. P. D. Abbatt and M. J. Molina, Physical Chemistry of the H_2SO_4/H_2O Binary System at Low Temperatures: Stratospheric Implications, *J. Phys. Chem.*, 1993, **97**(28), 7351–7358, available from: **https://pubs.acs.org/sharingguidelines**.

105 L. Yao, O. Garmash, F. Bianchi, J. Zheng, C. Yan, J. Kontkanen, *et al.*Atmospheric new particle formation from sulfuric acid and amines in a Chinese megacity, *Science*, **361**(6399), 278–281, available from: **https://www.science.org**.

106 F. Yu and G. Luo, Modelling of gaseous dimethylamine in the global atmosphere: impacts of oxidation and aerosol uptake, *Atmos. Chem. Phys.*, 2014, **14**, 17727–17748, available from: **https://www.atmos-chem-phys-discuss.net/14/17727/2014/**.

107 A. Kürten, New particle formation from sulfuric acid and ammonia: nucleation and growth model based on thermodynamics derived from CLOUD measurements for a wide range of conditions, *Atmos. Chem. Phys.*, 2019, **19**(7), 5033–5050, available from: **https://acp.copernicus.org/articles/19/5033/2019/**.

108 S. Yang, Z. Liu, P. S. Clusius, Y. Liu, J. Zou, Y. Yang, *et al.*, Chemistry of new particle formation and growth events during wintertime in suburban area of Beijing: insights from highly polluted atmosphere, *Atmos. Res.*, 2021, **255**, 105553, available from: **https://www.sciencedirect.com/science/article/pii/S0169809521001058**.

109 L. Yao, O. Garmash, F. Bianchi, J. Zheng, C. Yan, J. Kontkanen, *et al.*, Atmospheric new particle formation from sulfuric acid and amines in a Chinese megacity, *Science*, 2018, **361**(6399), 278–281, DOI: **10.1126/science.aao4839**.

110 P. Roldin, M. Ehn, T. Kurtén, T. Olenius, M. P. Rissanen, N. Sarnela, *et al.*, The role of highly oxygenated organic molecules in the boreal aerosol-cloud-climate system, *Nat. Commun.*, 2019, **10**(1), 4370, DOI: **10.1038/s41467-019-12338-8**.

111 J. Wildt, T. F. Mentel, A. Kiendler-Scharr, T. Hoffmann, S. Andres, M. Ehn, *et al.*, Suppression of new particle formation from monoterpene oxidation by NO_x, *Atmos. Chem. Phys.*, 2014, **14**(6), 2789–2804, available from: **https://acp.copernicus.org/articles/14/2789/2014/**.

112 X. Cheng, Q. Chen, Y. Jie Li, Y. Zheng, K. Liao and G. Huang, Highly oxygenated organic molecules produced by the oxidation of benzene and toluene in a wide range of OH exposure and NO_x conditions, *Atmos. Chem. Phys.*, 2021, **21**(15), 12005–12019, available from: **https://acp.copernicus.org/articles/21/12005/2021/**.

113 L. L. J. Quéléver, K. Kristensen, L. Normann Jensen, B. Rosati, R. Teiwes, K. R. Daellenbach, *et al.*, Effect of temperature on the formation of highly oxygenated organic molecules (HOMs) from alpha-pinene ozonolysis, *Atmos. Chem. Phys.*, 2019, **19**(11), 7609–7625, available from: **https://acp.copernicus.org/articles/19/7609/2019/**.

114 J. Hammes, A. Lutz, T. Mentel, C. Faxon and M. Hallquist, Carboxylic acids from limonene oxidation by ozone and hydroxyl radicals: insights into mechanisms derived using a FIGAERO-CIMS, *Atmos. Chem. Phys.*, 2019, **19**(20), 13037–13052, available from: **https://acp.copernicus.org/articles/19/13037/2019/**.

115 X. Fang, M. Hu, D. Shang, R. Tang, L. Shi, T. Olenius, *et al.*, Observational Evidence for the Involvement of Dicarboxylic Acids in Particle Nucleation, *Environ. Sci. Technol. Lett.*, 2020, **7**(6), 388–394, DOI: **10.1021/acs.estlett.0c00270**.

116 M. Kulmala, L. Dada, K. R. Daellenbach, C. Yan, D. Stolzenburg, J. Kontkanen, *et al.*, Is reducing new particle formation a plausible solution to mitigate particulate air pollution in Beijing and other Chinese megacities?, *Faraday Discuss.*, 2021, **226**, 334–347.

117 S. Tuovinen, J. Kontkanen, J. Jiang and M. Kulmala, Investigating the effectiveness of condensation sink based on heterogeneous nucleation theory, *J. Aerosol Sci.*, 2020, **149**, 105613.

118 A. Hamed, H. Korhonen, S. L. Sihto, J. Joutsensaari, H. Jrvinen, T. Petäjä, *et al.*, The role of relative humidity in continental new particle formation, *J. Geophys. Res.: Atmos.*, 2011, **116**(D3), DOI: **10.1029/2010JD014186**.

119 K. Wang, X. Ma, R. Tian and F. Yu, Analysis of new particle formation events and comparisons to simulations of particle number concentrations based on GEOS-Chem-advanced particle microphysics in Beijing, China, *Atmos. Chem. Phys.*, 2023, **23**(7), 4091–4104.

120 X. Li, S. Chee, J. Hao, J. P. D. Abbatt, J. Jiang and J. N. Smith, Relative humidity effect on the formation of highly oxidized molecules and new particles during monoterpene oxidation, *Atmos. Chem. Phys.*, 2019, **19**(3), 1555–1570.

121 H. Henschel, T. Kurtén and H. Vehkamäki, Computational Study on the Effect of Hydration on New Particle Formation in the Sulfuric Acid/Ammonia and Sulfuric Acid/Dimethylamine Systems, *J. Phys. Chem. A*, 2016, **120**(11), 1886–1896.

122 K. Wang, X. Ma, R. Tian and F. Yu, Analysis of new particle formation events and comparisons to simulations of particle number concentrations based on GEOS-Chem-advanced particle microphysics in Beijing, China, *Atmos. Chem. Phys.*, 2023, **23**(7), 4091–4104.

123 K. Lehtipalo, C. Yan, L. Dada, F. Bianchi, M. Xiao, R. Wagner, *et al.*, *Multicomponent new particle formation from sulfuric acid, ammonia, and biogenic vapors*, 2018, available from: **https://www.science.org**.

124 C. Rose, Q. Zha, L. Dada, C. Yan, K. Lehtipalo, H. Junninen, *et al.*, *Observations of biogenic ion-induced cluster formation in the atmosphere*, 2018, available from: **https://www.science.org**.

125 P. Paasonen, T. Olenius, O. Kupiainen, T. Kurtén, K. Kurtén, T. Petäjä, *et al.*, On the formation of sulphuric acid-amine clusters in varying atmospheric conditions and its influence on atmospheric new particle formation, *Atmos. Chem. Phys.*, 2012, **12**, 11485–11537, available from: **https://www.atmos-chem-phys-discuss.net/12/11485/2012/**.

126 S. Wang, R. Wu, T. Berndt, M. Ehn and L. Wang, Formation of Highly Oxidized Radicals and Multifunctional Products from the Atmospheric Oxidation of Alkylbenzenes, *Environ. Sci. Technol.*, 2017, **51**(15), 8442–8449.

127 J. Tröstl, W. K. Chuang, H. Gordon, M. Heinritzi, C. Yan, U. Molteni, *et al.*, The role of low-volatility organic compounds in initial particle growth in the atmosphere, *Nature*, 2016, **533**(7604), 527–531.

128 S. Yang, Z. Liu, P. S. Clusius, Y. Liu, J. Zou, Y. Yang, *et al.*, Chemistry of new particle formation and growth events during wintertime in suburban area of Beijing: insights from highly polluted atmosphere, *Atmos. Res.*, 2021, **255**, 105553.

129 V. Vakkari, P. Tiitta, K. Jaars, P. Croteau, J. P. Beukes, M. Josipovic, *et al.*, Reevaluating the contribution of sulfuric acid and the origin of organic compounds in atmospheric nanoparticle growth, *Geophys. Res. Lett.*, 2015, **42**(23), 10486–10493.

130 H. Man, Y. Zhu, F. Ji, X. Yao, N. T. Lau, Y. Li, *et al.*, Comparison of Daytime and Nighttime New Particle Growth at the HKUST Supersite in Hong Kong, *Environ. Sci. Technol.*, 2015, **49**(12), 7170–7178.

131 W. 4 Thomson, On the Equilibrium of Vapour at a Curved Surface of Liquid, *Proc. R. Soc. Edinburgh*, 1872, **7**, 63–68, available from: **https://www.cambridge.org/core/product/FE2D8D526BD8347E46274E63329AA521**.